CR-66954

STUDY FOR ADVANCED DEVELOPMENT OF 15-MICRON (Hg,Cd)Te DETECTORS

By Harris Halpert and Toivo Koehler
Honeywell Radiation Center

Prepared under Contract No. NAS 1-8996
Honeywell Radiation Center
Lexington, Mass.

for

NATIONAL AERONAUTICS AND SPACE ADMINISTRATION

FACILITY FORM 602
N70-32563 (ACCESSION NUMBER) (THRU) 1
87 (PAGES) (CODE)
CR-66954 (NASA CR OR TMX OR AD NUMBER) 26 (CATEGORY)

CR-66954

STUDY FOR ADVANCED DEVELOPMENT OF 15-MICRON (Hg,Cd)Te DETECTORS

By Harris Halpert and Toivo Koehler
Honeywell Radiation Center

Prepared under Contract No. NAS 1-8996
Honeywell Radiation Center
Lexington, Mass.

for

NATIONAL AERONAUTICS AND SPACE ADMINISTRATION

PRECEDING PAGE BLANK NOT FILMED.

TABLE OF CONTENTS

LIST OF FIGURES AND TABLES

LIST OF FIGURES AND TABLES (CONT.)

LIST OF FIGURES AND TABLES (CONT.)

STUDY FOR ADVANCED DEVELOPMENT OF 15-MICRON (Hg,Cd)Te DETECTORS

By Harris Halpert and Toivo Koehler
Honeywell Radiation Center

INTRODUCTION

A theoretical and experimental program has been undertaken to study 1/f noise in (Hg,Cd)Te with a peak response of 15 μm. The main purpose has been to develop high performance 15 μm (Hg,Cd)Te detectors for slow scan operation in radiatively cooled satellite applications requiring low bias power consumption. As a result of these requirements, the main emphasis has been to isolate the source of 1/f noise as either the contacts, surface, or bulk as a first step toward reducing 1/f noise in high resistivity material.

This report discusses the characteristics of 1/f noise, previous attempts to find a source and mechanism of 1/f noise in other materials, and the progress made in the understanding of 1/f noise in (Hg,Cd)Te.

CHARACTERISTICS OF 1/f NOISE

Frequency Spectrum of 1/f Noise

When direct current is passed through semiconductor material and the log mean square noise current is plotted vs log frequency,

we obtain the classic noise spectrum shown in Figure 1. Aside from the generation-recombination (g-r) noise found at intermediate frequencies and the thermal noise seen beyond the g-r rolloff, this spectrum exhibits low frequency excess noise. This noise which decreases rapidly with increasing frequency is known as 1/f noise. Actually, very few investigators find an exact 1/f law, usually the spectrum has the form $1/f^n$ where n can vary from 0.9 to 1.2.

No single simple physical process has been found that will give this characteristic 1/f noise spectrum. A flat spectrum or white noise can be obtained from the sum of many similar time independent events and a $1/f^2$ spectrum can be obtained from the high frequency portion of the g-r noise where $\omega \tau >> 1$, but a spectrum intermediate between these two (i.e., 1/f) has been difficult to synthesize from a single elementary process.

It has been shown by Vander Ziel[1] that the 1/f law, however, cannot hold in the whole frequency range. If a fluctuating quantity X(t) is defined for $0 < t < t$, we obtain from the Wiener-Khinchin theorem the fact that:

$$F(f) = 4 \overline{X(t)^2} \int_0^\infty c(t') \cos \omega t' \, dt' \qquad (1)$$

where F(f) is the resulting power spectral distribution function and c(t') is the normalized correlation function such that:

$$c(t') = \overline{X(t)\, X(t + t')} \Big/ \overline{X(t)^2}$$

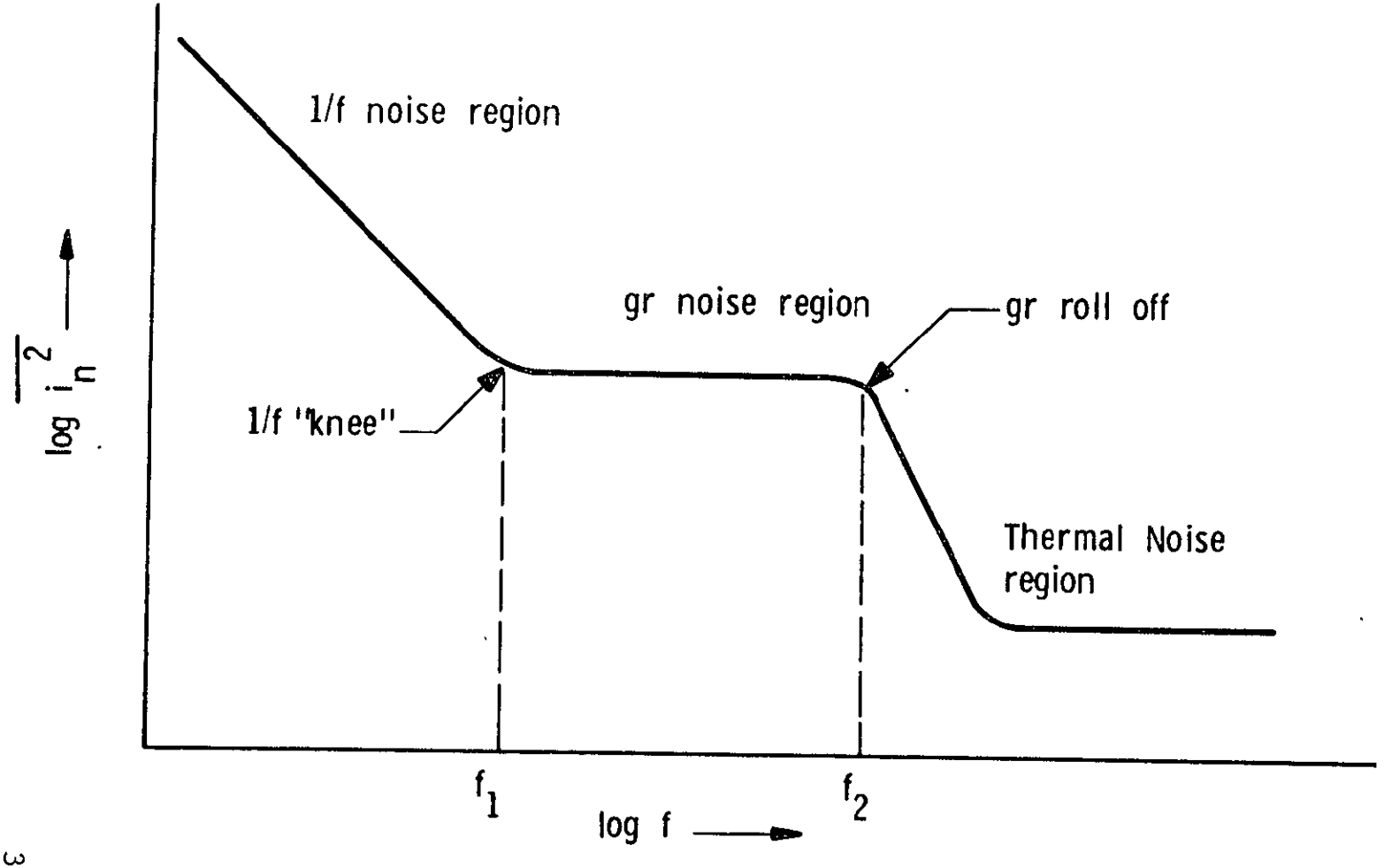

Figure 1 CLASSIC NOISE SPECTRUM

$c(t') = 1$ for $t' = 0$, $c(t')$ is independent of t and $c(t') = 0$ when $/t/ \gg \tau$, where τ is the correlation time. In the case of fluctuating quantities which are caused by a large number of independent events occurring at random, τ is the duration of the event; in the case of fluctuations involving decay problems τ measures the average lifetime of the decay.

$F(f)$ cannot satisfy a $1/f$ spectra for all frequencies, i.e., $0 < f < \infty$ for according to a well known Fourier theorem, we can reverse Equation (1) such that:

$$\overline{X(t)\ X(t + t')} = \int_0^\infty F(f) \cos 2\pi f \omega \, df$$

The autocorrelation function has to be a bounded continuous function which converges for all values of t'. Thus, $F(f)$ has to vary slower than $1/f$ for low frequencies and faster than $1/f$ for high frequencies.

Shot or g-r noise has a correlation function which is dependent upon one correlation time τ and gives a frequency dependence of:

$$F(f) = \text{constant} \times \frac{\tau}{(1 + \omega^2 \tau^2)}$$

$F(f)$ is then independent of frequency if $\omega \tau \ll 1$ and is proportional to $1/f^2$ for $\omega \tau \gg 1$. This is quite different from a $1/f$ law.

It is difficult to find a single event which gives rise to a correlation function such that the $1/f$ law is the result of it.

The most successful procedure in synthesizing a 1/f spectrum has arisen from the superposition of many shot or g-r spectra. If a continuous distribution of correlation times τ is introduced where $dP = g(\tau)d\tau$ represents the probability of a correlation time between τ and $\tau + d\tau$ and,

$$g(\tau) = 0 \quad \tau_1 > \tau > \tau_2$$

$$g(\tau) = 1/\tau \quad \tau_1 \leq \tau \leq \tau_2$$

Then,

$$F(f) = 4\,\overline{X(t)^2} \int_0^\infty \tau\,(1 + \omega^2\tau^2)^{-1}\, g(\tau)\, d\tau = \int_{\tau_1}^{\tau_2} \frac{d\tau}{1 + \omega^2\tau^2}$$

$$= \frac{A}{\omega}\,(\tan^{-1}\omega\tau_2 - \tan^{-1}\omega\tau_1)$$

If in the frequency range under consideration $\frac{1}{\tau_1} >> \omega >> \frac{1}{\tau_2}$ then,

$$F(f) \alpha\ 1/f$$

with the assumption that this law is valid in a restricted frequency region, determined by upper and lower cut-off times τ_2 and τ_1. Thus, to attain a 1/f spectrum, the probable frequency of τ must then be proportional to $1/\tau$ between τ_2 and τ_1.

Experimental attempts to find the upper and lower frequency limits of 1/f noise in semiconductor devices has yielded a wide range of frequencies where 1/f noise is applicable. By using

elaborate tape recording techniques, the low frequency portion of the spectrum has been investigated in various semiconductor devices. The 1/f law has been found to be valid down to 5×10^{-5} Hz in silicon and germanium rectifiers by Firle and Winston[2] and down to 2.5×10^{-4} Hz in germanium filaments by Rollin and Templeton[3]. Hyde[4] observed 1/f noise in two terminal germanium crystals up to 4 MHz and found a change-over to a $1/f^2$ spectrum above that frequency. Other authors have reported measurements on single crystal germanium filaments which indicate a departure from the 1/f law at high frequencies[5,6,7]. Bess and Kisner[7] noticed changes to a $1/f^2$ dependence at frequencies as low as 480 Hz for an etched germanium filament (n-type, roughly 30 Ω-cm) with a CCl_4 ambient and 570 Hz for the same sample in air ambient after it had aged for two weeks. Nevertheless, the wide range of frequencies over which the 1/f noise law holds had made it difficult to find a mechanism which could be related to time constants present in the solid.

General Characteristics of 1/f Noise

One of the first measured properties of 1/f noise was its dependence on current. The noise power was proportional to the square of the current for germanium filaments[8]. Although deviations from an I^2 law have been noted, the current dependence is generally a square law, characteristic of conductivity fluctuations. A direct experiment has substantiated the current dependence. Brophy and Rostoker[9] measured the noise from Hall effect probes as a function of magnetic field. Since dc Hall voltages are used to determine the average carrier density in semiconductors, the Hall noise voltage was interpreted in terms of carrier fluctuations. The results indicated that the 1/f noise behaves as a conductivity modulation.

1/f noise is characterized by the property that it has been found to be quite temperature invariant in several different devices. Montgomery[8] has found this to be true also in germanium. This temperature invariance over a wide range of temperatures has raised questions as to the validity of many mechanisms (especially diffusion and slow surface state models) proposed for 1/f noise.

Montgomery[8] has found that 1/f noise in germanium filaments tends to increase with resistivity. He came to the conclusion that the ratio of 1/f noise to Johnson noise at constant bias voltage tends to be independent of the resistivity of the crystal. Measurements by MacRae and Levinstein[10] in gold doped germanium substantiated Montgomery's conclusion that,

$$< v^2 > = \frac{\alpha\, RV^2}{f}$$

where V is the bias voltage and α some experimentally determined constant.

SOURCES OF 1/f NOISE

Introduction

From the results of the 1/f noise frequency spectrum, the problem of 1/f noise is reduced to finding a physical process that gives rise to a distribution function proportional to $1/\tau$ over an appropriate range of time constants. Although electronic transitions between traps and the conduction and valence bands may give long

trapping times, such a distribution cannot arise from these transitions. Under these conditions, the shortest time constant would dominate the noise spectrum, since it is the fastest process that determines the average lifetime of a free carrier. This is the main reason that 1/f noise cannot be caused by a superposition of g-r noise terms involving deep traps.

Brophy[12] demonstrated that 1/f noise also occurs when conductivity changes are detected by placing the crystal in a temperature gradient rather than in an electric field. If we presume as Brophy did that the noise is not inherent in the passage of current but can be attributed to conductivity fluctuations, there are two alternatives: either the carrier densities themselves are modulated (e.g., by the random creation and disappearance of donor centers) or the rates of the carrier transitions are modulated in some way. Therefore, the problem of 1/f noise is that of finding a mechanism or mechanisms which satisfactorily explains these conductivity modulations with the necessary distribution function to give a 1/f spectrum between appropriate frequency limits.

Noise Sources

General - There are three possible sources of 1/f noise, the contacts, the surface, or the bulk of the material. Contact noise can be bypassed through the use of voltage sidearm probes and it is assumed that the remaining low frequency noise is characteristic of the filament itself. There is extensive experimental evidence to show that 1/f noise, at least in germanium, is predominantly a

surface phenomena, although it should be noted that not all 1/f noise originates from the surface. Probably, the most direct proof for the surface dependence of 1/f noise was given by Maple, Bess, and Gebbie[11] who found a 10 to 20 dB increase in 1/f noise by switching the filament from a dry nitrogen ambient to one of carbon tetrachloride. Montgomery[8] found that in germanium, a sandblasted surface usually gives the lowest noise while etching could raise the noise voltage by a factor of ten or more, though the dc resistance changed only a few percent. He also could produce changes in 1/f noise by concentrating the carriers on the surface by means of a magnetic field.

The Surface - The basic model of a semiconductor surface has emerged from studies made for the most part on germanium and silicon surfaces. A fundamental energy level diagram of the surface is shown in Figure 2. From the point of view of its electronic behavior, the surface may be roughly divided into three separate regions: the space-charge layer, associated with surplus or deficit of free carriers of thickness 10^{-5} cm or greater; the surface proper consisting of the first few atomic planes of the semiconductor; and, in the case of a real surface, an adsorbed layer of foreign material. In a semiconductor such as germanium or silicon, this last consists mainly of an oxide film, usually 10-30 Å thick, together with various species adsorbed from the etchant and the surrounding ambient. The oxide film is shown next to the semiconductor, the midgaps of the two materials having been assumed to lie at the same energy level.

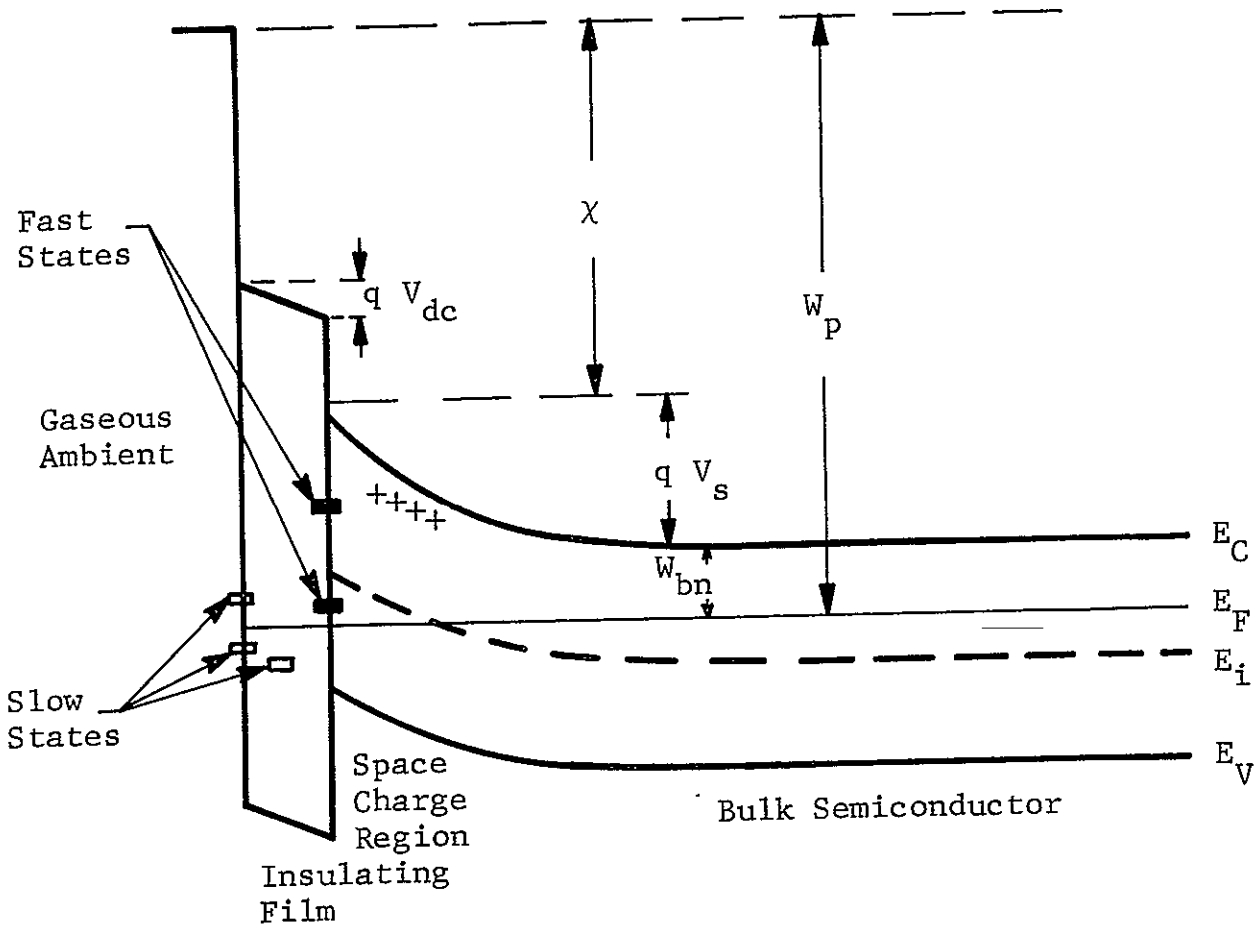

Figure 2 TYPICAL SEMICONDUCTOR SURFACE

The fundamental variable characterizing the space-charge layer is the barrier height V_s (or surface potential) which, for given bulk conditions, determines uniquely the shape of the potential barrier and the carrier distribution in this region. The surface proper and the adsorbed layer are usually the sites of localized electronic states - the surface states. These are known to be sensitive to mechanical and chemical treatment and to the gaseous or liquid environment to which the surface is exposed. In germanium and silicon, the surface states can be divided into two distinct categories, according to whether the transition times between the states and the underlying bulk are very short (microseconds or less) or very long (seconds or more). The former, the fast states, are in intimate contact with the semiconductor bulk, and are probably located at, or very close to, the semiconductor/oxide interface. The latter, the slow states, are associated with the oxide and adsorbed species and are known to be distributed within the oxide film and/or on its outer surface. Another fundamental entity characterizing the surface is the work function W_p. This is the sum of the energy parameter $W_{bn} = E_c - E_f$, the barrier height $-qV_s$, and the electron affinity χ.

When the majority carrier density in the space charge region is greater than that in the bulk, the space charge region is termed an accumulation layer. An inversion layer is formed if the minority carrier density at the surface is greater than the majority carrier density in the bulk. If the majority carrier density at the surface and the minority carrier density at the surface are both less than the majority carrier density in the bulk, we refer to a depletion layer.

The nature of the surface states was particularly investigated with the aid of the field effect. In this effect the conductivity of the germanium sample is modulated by changing the surface charges with the aid of a pulsed or sinusoidally modulated transverse electric field (perpendicular to the surface). If a pulsed field is applied, there is first a relatively rapid response, reaching a value corresponding to some quasi-equilibrium state of the carriers and the surface recombination centers. Then the conductance decays slowly to its original value with a half life for the decay ranging from milliseconds to several seconds, depending on the surface treatment and the gaseous ambient. The effect has been generally analyzed assuming that the "fast states" are responsible for the recombination velocity of the carriers and the "slow states" give the tail in the response curve.

McWhorter assumes that free carriers communicate with the slow states by tunneling through the barrier. The attractive feature of this assumption is the temperature independence of this process. McWhorter measured the response to a sinusoidally varying field. In many cases the response could be approximated by,

$$\Delta \sigma \ (\omega) = a \log b \ \omega \qquad (2)$$

for frequencies $f < f_{max}$. If the slow surface states would have a single capture time constant τ, then McWhorter shows that the response should be of the form $\frac{j \ \omega \ \tau}{1 + j \ \omega \ \tau}$.

The form (2) can only be explained if we introduce a distribution of τ's.

$$\Delta \sigma (\omega) = a' \int_{\tau_1}^{\tau_2} \frac{g(\tau)\, j\, \omega\, \tau}{1 + j\, \omega\, \tau}\, d\tau$$

For $g(\tau) \approx 1/\tau$ the result (2) is approximately found. Apparently, this is just the distribution of time constants needed to obtain 1/f noise. It is accordingly very promising to assume that 1/f noise is caused by spontaneous fluctuations in the capture and release of carriers by the slow surface states. Unfortunately, the field experiments seem to indicate an upper value of f_{max} lower than usually found for 1/f noise.

Bess[15,16] has proposed an entirely different interpretation of 1/f noise. In accordance with the observation that the amount of 1/f noise can be changed by plastic deformation, Bess assumed that the noise was associated with edge dislocations. Impurities should be diffusing along the edge dislocation line to and from the surface where they undergo some type of Brownian motion. With a highly specialized mathematical model, this results in 1/f noise. Although Bess' theory per se may be doubtful, some of his ideas have been used by others. Morrison[17] pointed out that the energy band structure in the neighborhood of a dislocation is similar to that of the surface and a fluctuation of the trapped charge will thus modulate the dislocation potential and the recombination velocity yielding a 1/f spectrum. Jantsch[18,19] has studied 1/f noise in silicon and he proposes a theory where 1/f noise is produced by a modulation of surface recombination. In this theory,

chemisorbed water on an etched silicon surface acts as the slow states and are directly situated at the interface of the silicon and oxide layers. Also the chemisorbed water itself acts as a fast surface state and consequently as a recombination center. The chemisorbed molecules dissociate from their active centers and diffuse in the interface of the surface by Brownian motion until they are bonded again. During the removal of a chemisorbed molecule from an active center, a chemical bond is interrupted and surface recombination is modulated.

His model was partially based on the experiments of Sah and Hielscher[20] who showed that the intensity of 1/f noise is proportional to the number of fast surface states in silicon MOS devices and partially upon his own experiments[19] which showed a relation between 1/f noise current and the dc current of an alloyed silicon diode biased in the reverse direction, since reverse current is generated at surface recombination centers. Such a theory is not in opposition to the experiments of MacRae[21] who found that removing slow surface states in silicon by vacuum cleaning did not affect the magnitude or spectrum of 1/f noise.

Field effect experiments performed in germanium by MacRae and Levinstein[22] showed an increase in 1/f noise associated with an inversion layer at lower temperatures. The magnitude of the 1/f noise depended upon the ambient, increasing with a decrease in the slow state relaxation time. An investigation of the relaxation processes associated with the charge transfer between the bulk and slow surface states after the application of the dc electric field

revealed a 1/f noise relaxation which was independent of the mode of the conductivity relaxation. The noise relaxed back to its original value with a logarithmic time dependence characteristic of a $1/\tau$ distribution in time constants and the conductance decayed with a combination of exponential and logarithmic terms depending on the surface conditions.

Some of the more recent theories of 1/f noise have shown much promise, but the exact source and mechanism of 1/f noise is still uncertain.

STUDY OF 1/f NOISE IN 15 μm (Hg,Cd)Te

Background

Fifteen micron (Hg,Cd)Te has been found to exhibit a classic noise spectrum where the low frequency performance is limited by the 1/f noise voltage. Previous work[23] performed at the Honeywell Radiation Center has established the relationship between 1/f noise, the bias current and the sample resistivity. Figure 3, a plot of 1/f noise voltage vs bias current in (Hg,Cd)Te, shows that β the exponent of the bias current, equals 2. This current dependence suggests that 1/f noise in (Hg,Cd)Te is the result of carrier density fluctuations as was seen in other semiconductors.

Kruse et al[13] have defined a 1/f noise constant such that:

$$\overline{V_{1/f}^2} = \frac{K_1 I^2 R^2 \Delta f}{f^\alpha} = \frac{C_1}{\ell A} \frac{I^2 R^2}{f^\alpha} \Delta f$$

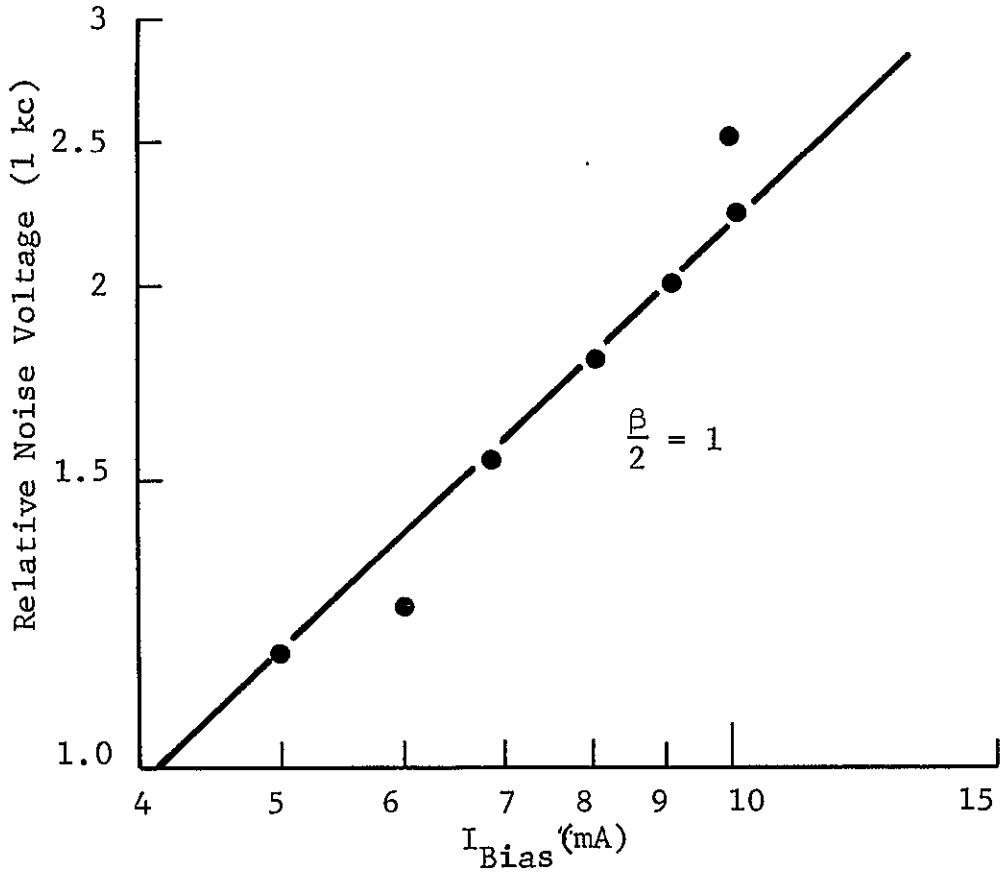

Figure 3 NOISE VOLTAGE VS BIAS CURRENT IN 15 MICRON (Hg,Cd)Te

where,

C_1 is a factor dependent upon material but independent of dimensions; ℓ the detector length and A the cross-sectional area;

I is the bias current;

R is the sample resistance;

Δf is the electrical bandwidth;

β is the exponent of the frequency dependence which is approximately 2.

The noise voltage can be expressed in terms of the element resistivity ρ. Thus,

$$\overline{v_{1/f}^2} = \frac{C_1 \rho^2 I^2 \ell}{f A^3} \Delta f$$

so that,

$$C_1 = \frac{V^2 f A^3}{\rho^2 I^2 \ell \Delta f}$$

The noise constant C_1 has been found to be dependent upon resistivity to the 5/2 power when C_1 is plotted against ρ as in Figu 4. This makes the noise voltage dependent upon approximately the square of the sample resistivity and says that low resistivity (Hg,Cd)Te detectors will exhibit low 1/f. However, the source of 1/f noise in (Hg,Cd)Te has not been found and the main emphasis of the present study has been to isolate the source as contacts, surface or bulk.

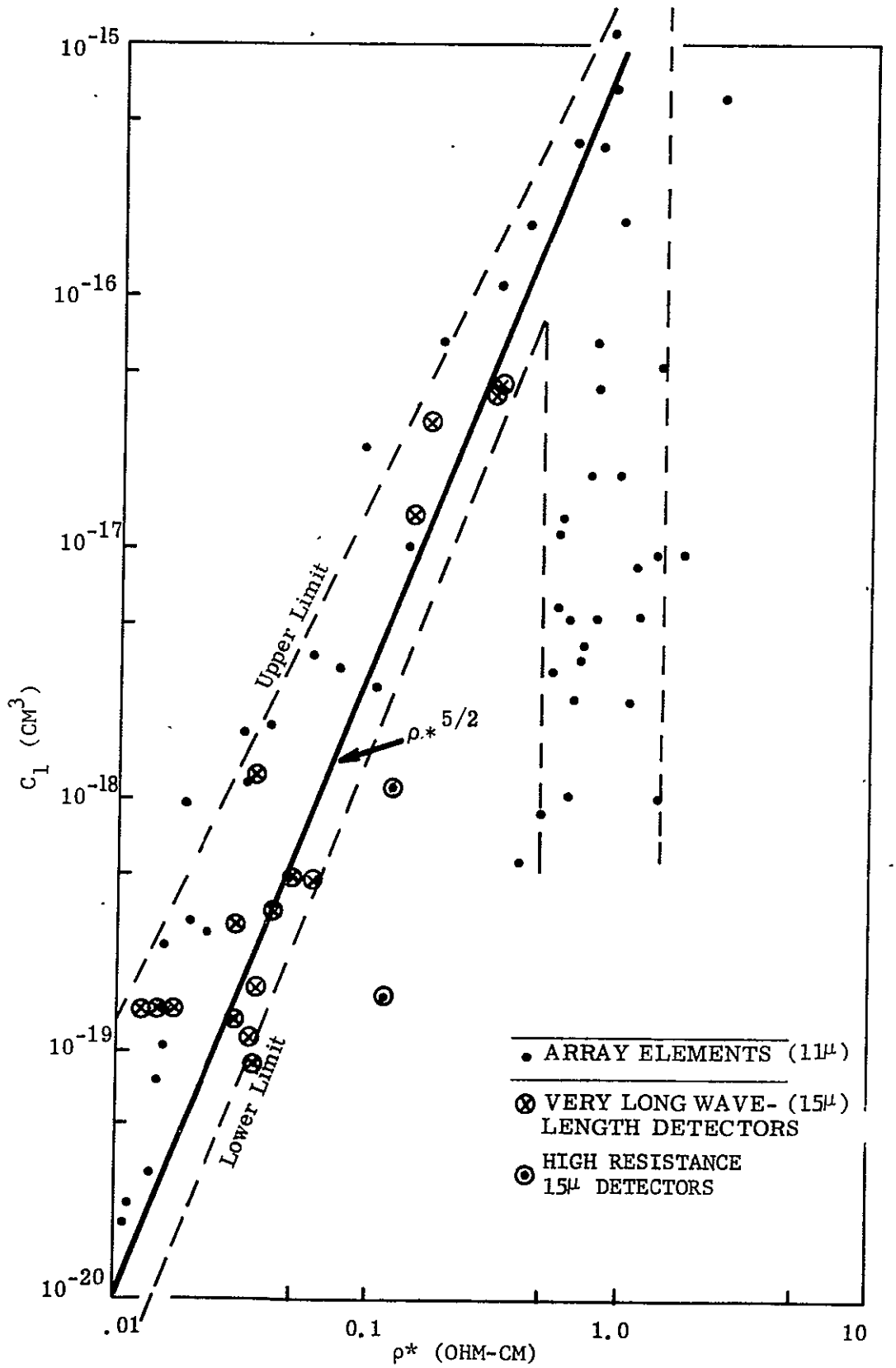

Figure 4 1/f COEFFICIENT VS RESISTIVITY

Material Inventory

Ingot Information - The ingot grown especially for this study was grown in the Material Preparation Laboratory at our Lexington facility. The design goals for the ingot were:

$\tau = 1\ \mu s$

$\mu = 2 \times 10^5\ cm^2/v\text{-}s$

$\eta = 5 \times 10^{13}\ cm^{-3}$

$x = 0.185\ (\lambda_{peak} = 15\ \mu)$

The slabs were indexed by their millimeter distance from the seed end (see Figure 5) and every 20 mm a slab was extracted for Hall measurements and slab parameters. The results of this evaluation are shown in Table I while Figures 6 and 7 are illustrations of the samples used for Hall measurements and later for 4-contact experiments. Since the Hall samples were 25 μm thin, they could be used as detectors and their noise spectra and detectivity information noted. Responsivity curves were made for many samples and a typical response curve is shown in Figure 8. The slabs were also thermal probed at 77 °K for type n or p and Figure 9 summarizes the thermal probe results.

Noise spectra were taken for a large number of slabs and representative results are shown in Figure 10. We see that the ingot exhibited high 1/f noise making it adequate for 1/f noise studies.

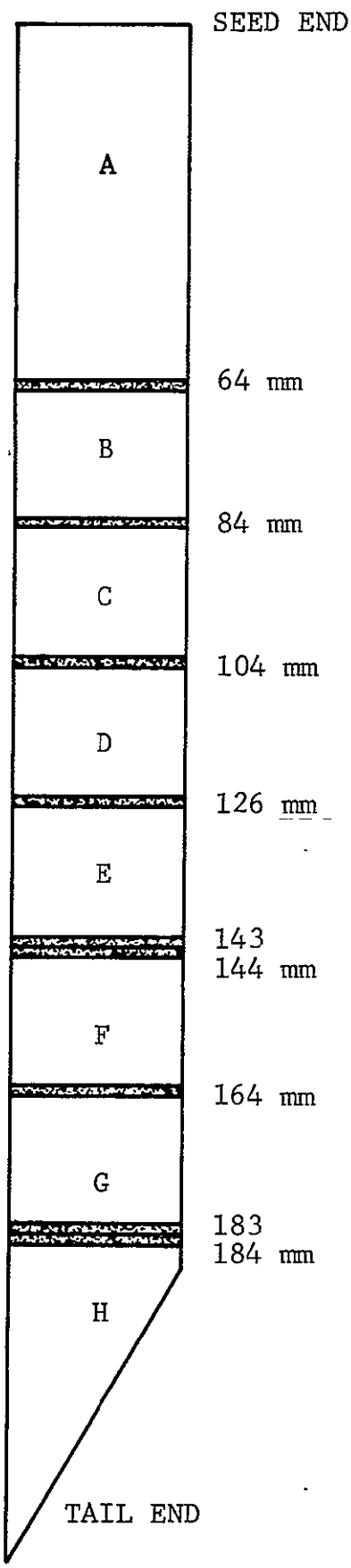

Figure 5 SLAB LOCATIONS

TABLE I
1/f MATERIAL INVENTORY FOR HALL DATA AT 77 °K

Slab	Sample No.	t	ρ	n	μ
		(μm)	(Ω cm)	(cm^{-3})	(cm^2/V.s)
S 125 E anneal		20	0.420	7.46×10^{14}	2×10^4
S 146 E anneal		17	0.493	1.02×10^{15}	1.24×10^4
S 126	3	940	0.181	*2.2×10^{14}	1.58×10^5
	2	940	4.6	*4.67×10^{14}	2.92×10^3
S 143	4	920	0.0198	2.09×10^{15}	1.51×10^5
	3	920	0.577	2.34×10^{14}	4.62×10^4
	2	920	1.66	2.62×10^{14}	1.44×10^4
S 164	2	850	0.515	2.48×10^{14}	4.89×10^4
S 152	5	25	3.29	1.60×10^{14}	1.18×10^4
	4	25	0.495	2.62×10^{14}	4.83×10^4
	3	25	0.0322	9.54×10^{14}	2.04×10^5
	2	25	0.00217	5.53×10^{15}	5.20×10^5

* Hall data partially n type and partially p type.

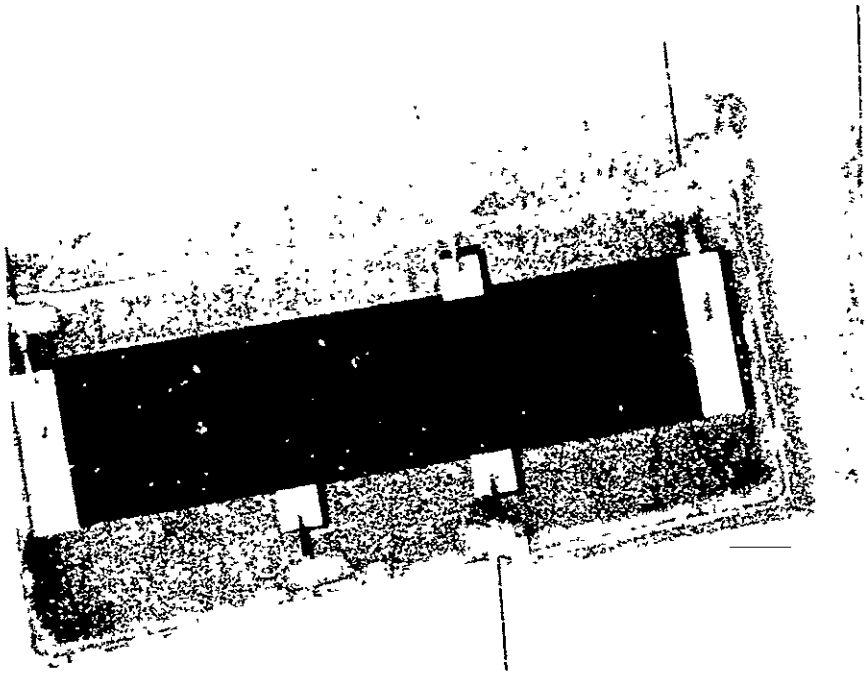

Figure 6 HALL SAMPLE PHOTOGRAPH

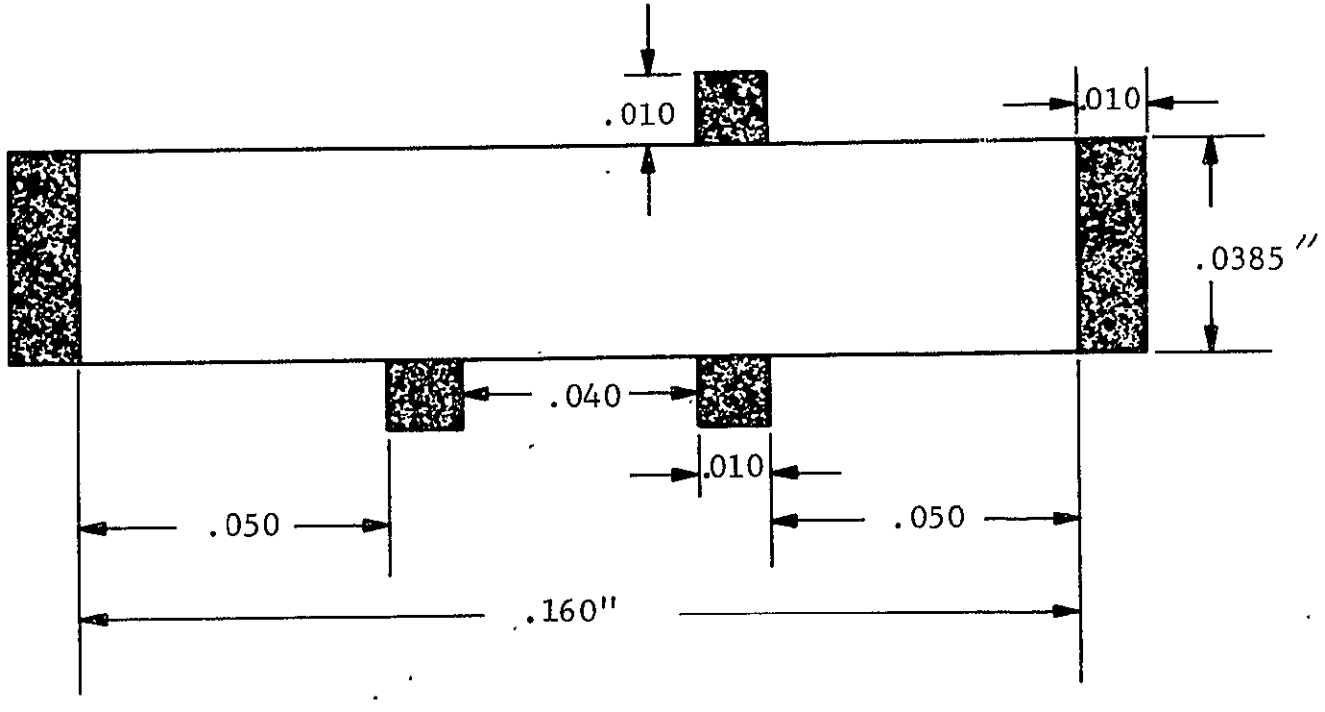

Figure 7 HALL SAMPLE DIMENSIONS

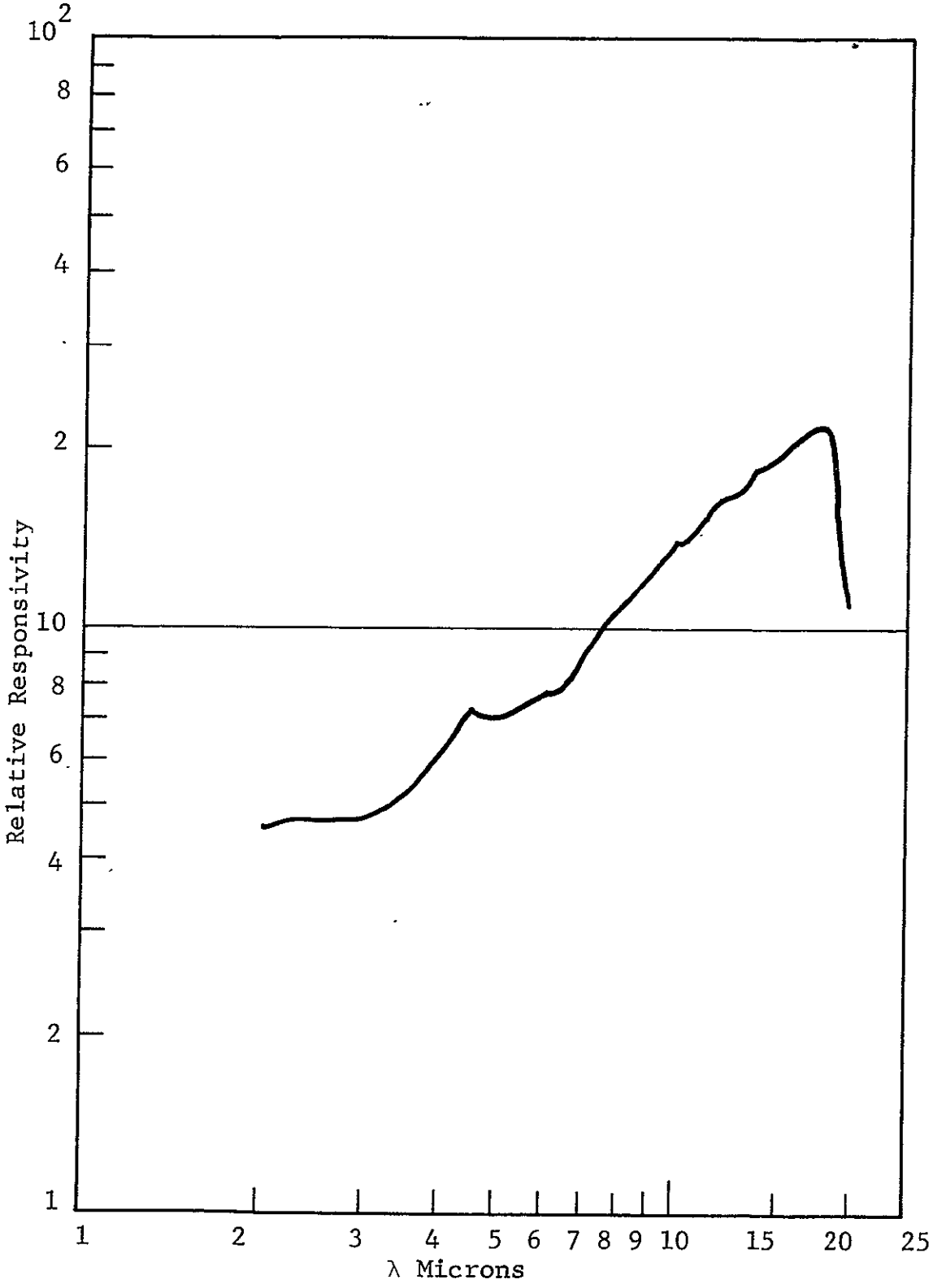

Figure 8 TYPICAL SPECTRAL RESPONSIVITY

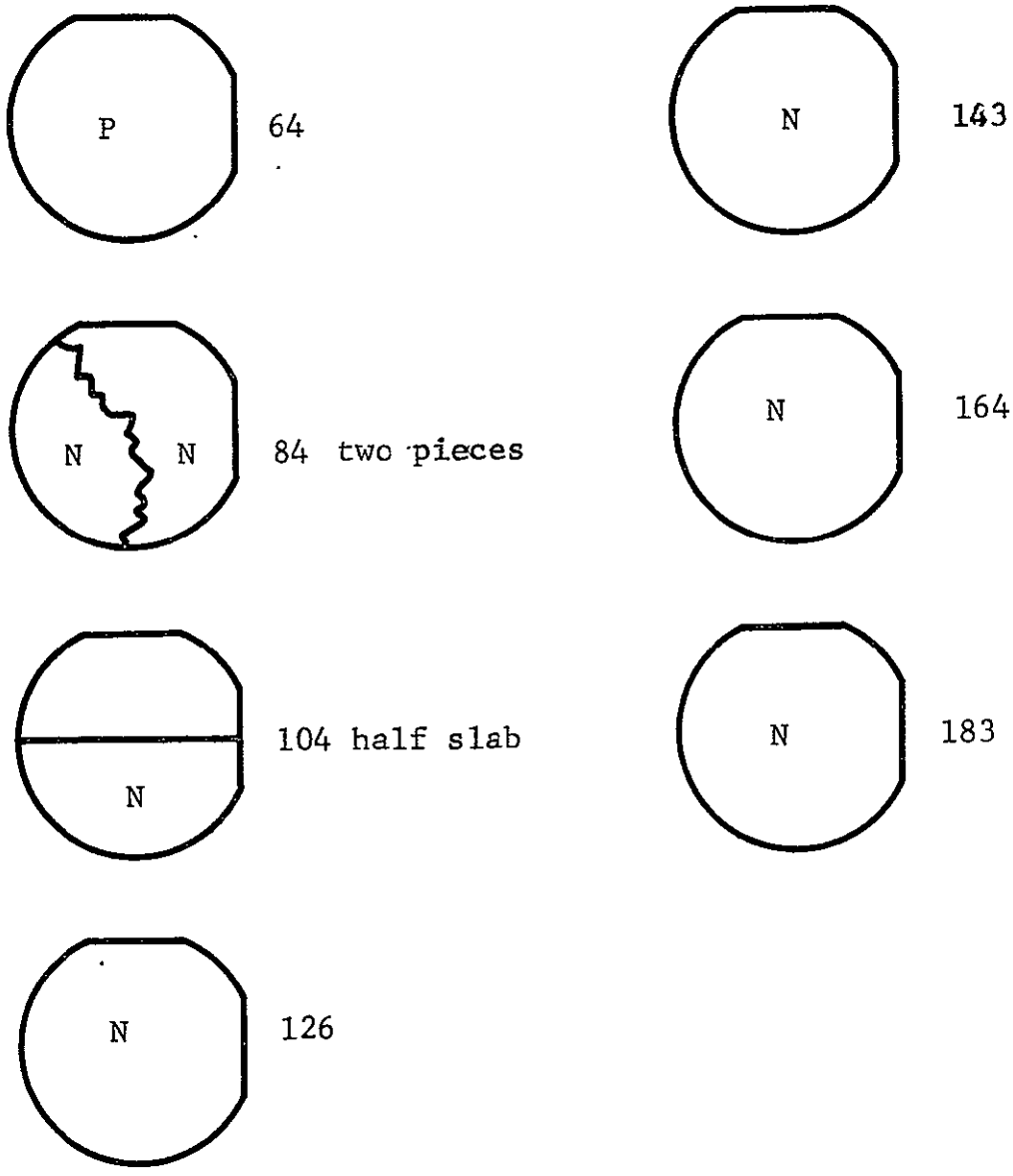

Figure 9 THERMAL PROBE RESULTS

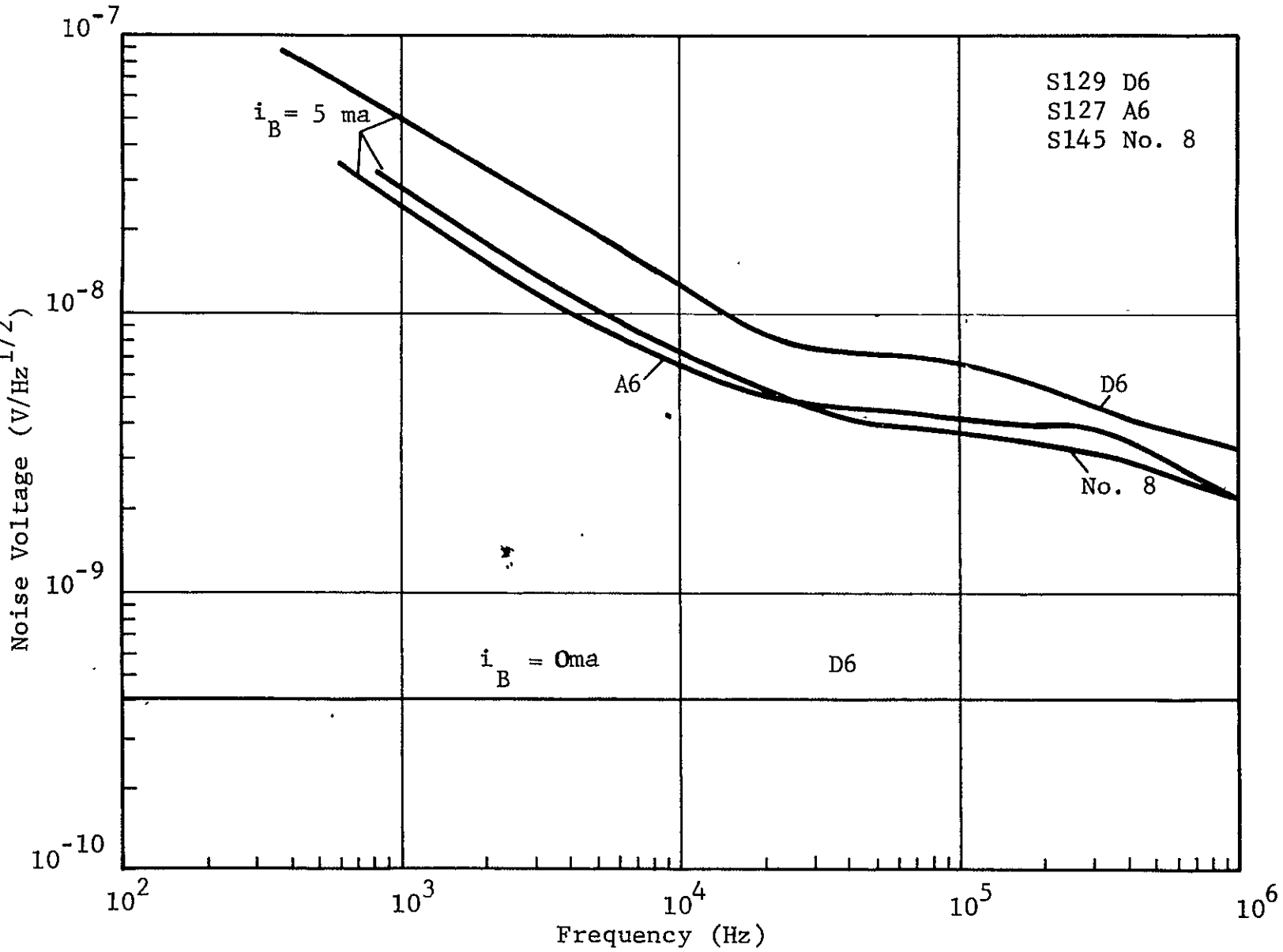

Figure 10 REPRESENTATIVE NOISE SPECTRA

We see from the responsivity curve that λ_{peak} is very close to 15 μm - the desired value. However, the purity and lifetime (≈ 140 -200 ns) fall short of the design goals. Attempts to improve n are discussed in the section on annealing. The ingot was adequate for single element 1/f noise studies requiring 15-μm material, however, we found the material homogeneity to be poor. This made comparisons across a slab or between adjacent slabs difficult, and this problem hampered our efforts throughout the program.

Hi ρ Material - Toward the end of the program, two high resistance slabs were obtained. The Hall data for samples from slab 152 are listed in Table I while in Table II a summary of resistivity, λ_{peak}, and λ cut-off are given for all detectors fabricated from both slabs 144 and 152. We see that S 152 exhibits extremely high ρ not only in the detectors but in the Hall data as well. Resistivity as high as 3.29 Ω-cm has been found for the fifth Hall sample with a carrier concentration of 1.6×10^{14} (one of the lowest seen at HRC). However, the peak response of these detectors ranges only from 10 μm to 12.5 μm. Nevertheless, this high resistance allowed us to study 1/f noise in high resistivity material. The results of this study are discussed in a subsequent section of this report.

Special Fabrication and Treatment Techniques

Bulk Treatment (Anneals) - The slab is annealed in a quartz ampule with a side arm filled with free mercury. The slab is heated to some temperature for a time t(h). The mercury is at another temperature T_2 to maintain a positive vapor pressure on the sample and

TABLE II
HALL DATA

Slab	Sample	Resistance (Ω) +	Resistance (Ω) -	λp (μm)	λco (μm)
152	A13	55.7	50.7	9.0	10
	A12	356	302	10	11
	A11	239	238	10	11
	A10	474	538	10	11
	A9 (PV)	334	538	11	11.5
	A8	328	278	11	13
	A7	34	34	12.5	14.5
144	B5	107		12	14.5
	B7	132		11	13
	B8	188		10.5	11.8
	B9	248		10	11.4
	D4	23		12	14.5
	D5	122		12	14.5
	D6	132		11	13.9
	D7	122		10	12.8

reduce the diffusion of mercury to the slab surface. Hence, each anneal can be characterized by a slab temperature (Ts), mercury temperature (Thg), and time t.

Honeywell has performed annealing experiments in the past on 8-14 μm (Hg,Cd)Te material. This work, supported under the Air Force Contract AF33(615)36F6 S/A No. 1 (6F-3421) Project No. 4056, Task No. 40562, concluded that annealing improved poor material D^*_{BB} in the "1/f" noise limited frequency range (1 kHz). Material which already exhibited high performance showed little change.

Anneal E, which was considered the standard, showed the best results for converting material from p-type to n-type and for increasing electron density due to the diffusion of Hg into the slab. Upon cooling, the Hg again diffuses out leaving an intrinsic layer at the surface of the slab. Two slabs (125 and 146) were put through the standard E annealing cycle, and Hall data was taken and is summarized in Table I. Direct comparison of the E annealed sample (S 125) with its adjacent unannealed slab (S 126) is impossible due to the partially p-type nature of the Hall data of S 126. Direct comparison of the Hall data of the other E annealed sample (S 146) with its adjacent unannealed slab S 143 yields nothing conclusive due to the material inhomogeneity. This problem hampered our annealing studies from the outset. We shall deal with this problem at a later point in the report.

Surface Treatment (etches) - Assuming the 1/f noise is due to adsorbed molecules at the surface and their resulting surface states,

it is a reasonable procedure to test this hypothesis using various etches to change the surface properties. For example, the standard proprietary etch, may leave residual chemicals on the surface. Removing these chemicals with a post etch or using a different etch may give an entirely different 1/f noise spectrum. Of course, the adsorbed molecules may not be from the etch at all. It may be nitrogen or oxygen from the atmosphere. Ambient gas cycle experiments have been performed in which the 1/f noise magnitude was changed[6].

Assuming residual chemicals to be the cause of 1/f noise, the following experiment was performed. Slab 127 was fabricated into vertical rows of detectors up to the etching step.

Table III summarizes the etches considered for the experiment. Row B was etched as a control strip with the standard etch (No. 1). Row A was etched with the standard etch, followed by a post etch of HNO_3 (HCl (No. 2). Row C was etched with No. 3. Data from Rows A and B are summarized in Figures 11 and 12.

TABLE III
ETCHES CONSIDERED

Etches	
1. Standard proprietary etch	wash in methanol
2. Standard proprietary etch followed by HNO_3 & HCl 1:1	wash in methanol
3. HF, HNO_3, Acetic Acid, Citric Acid 1:3:4:saturated.	

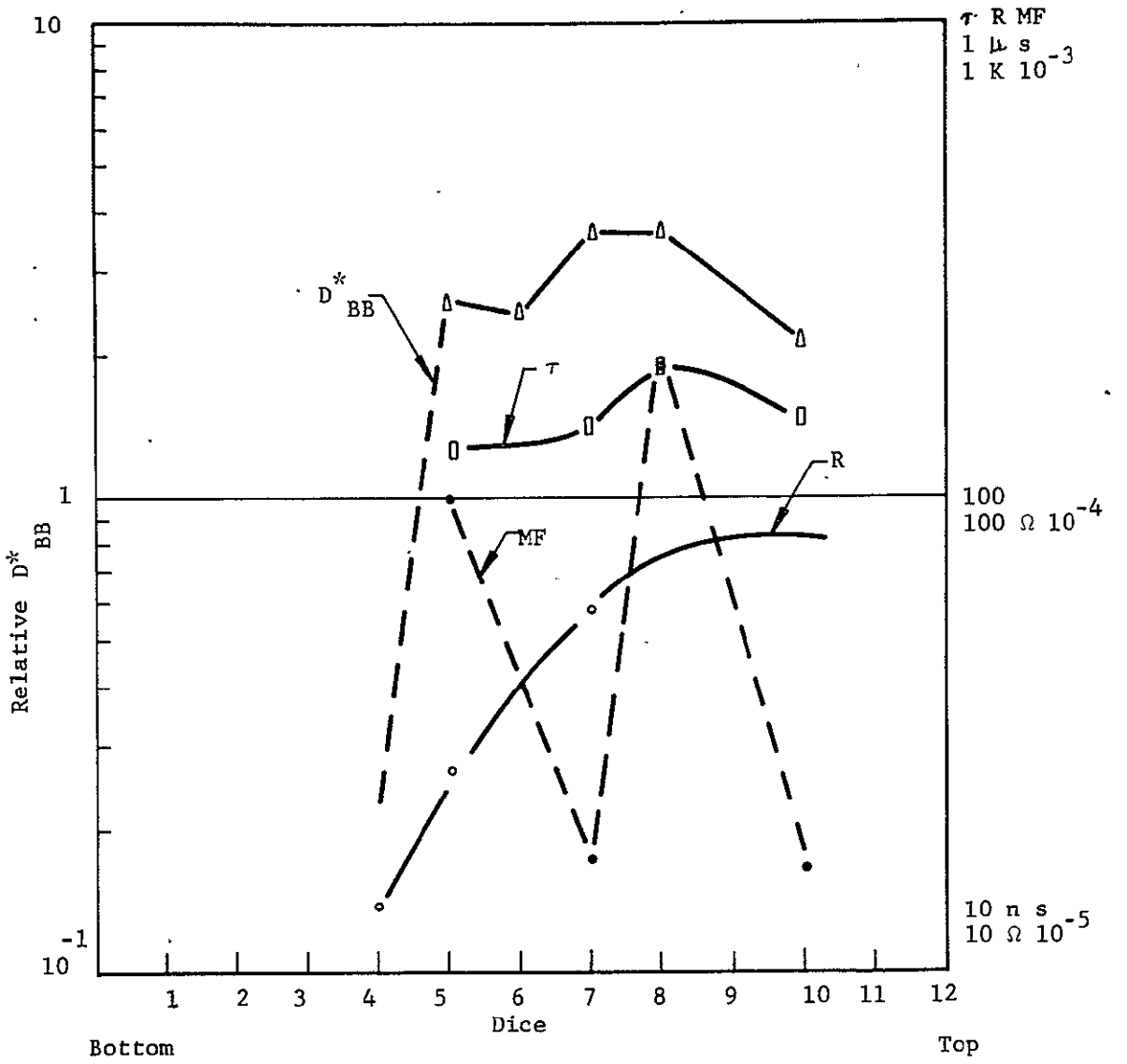

Figure 11 ROW A STANDARD ETCH + HNO_3, HCl 1:1

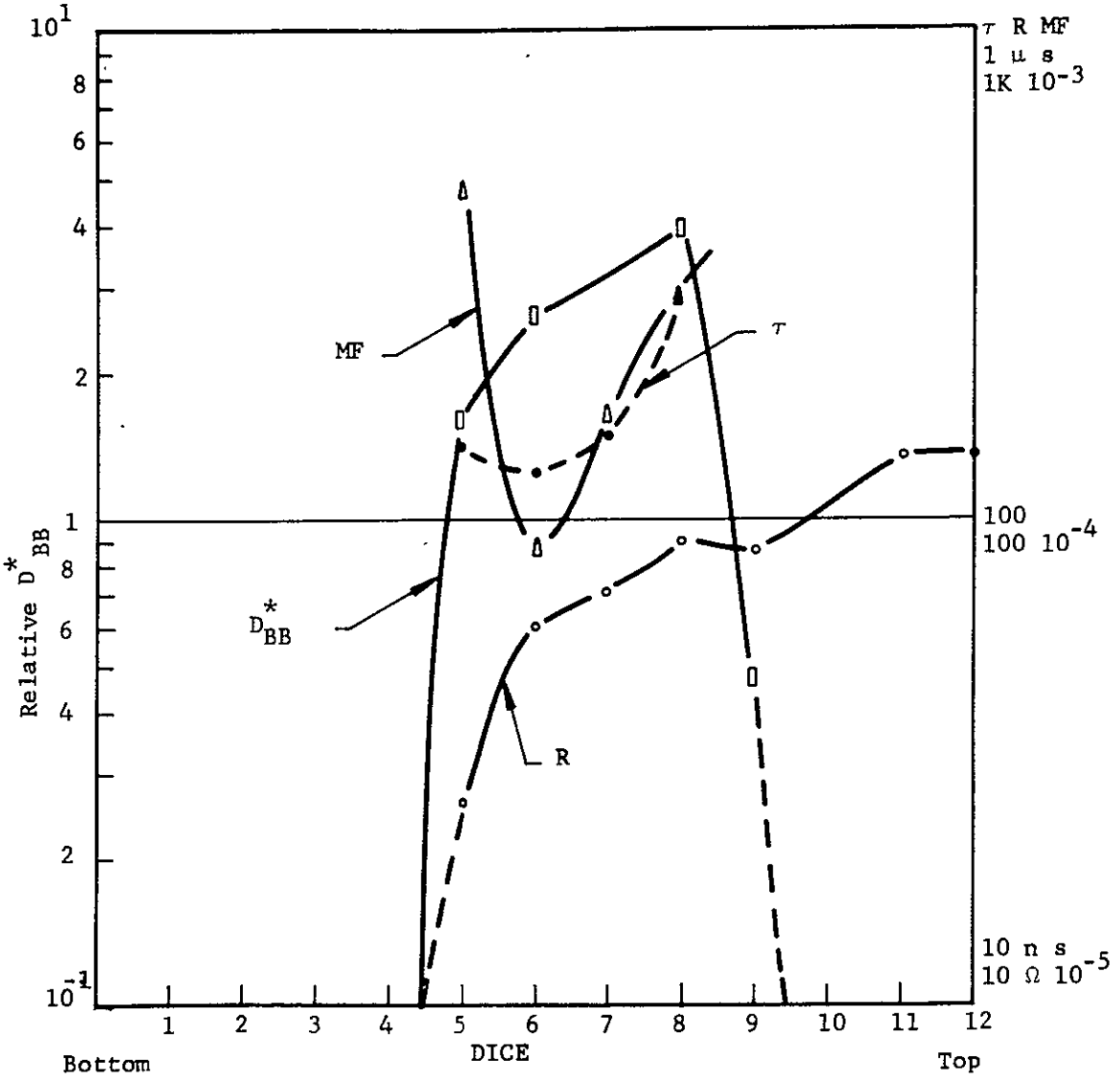

Figure 12 ROW B STANDARD ETCH

In this experiment, the figure of merit (MF) is used to evaluate the noise performance of various detectors. For background limited performance (BLIP) the device must be g-r noise limited. The figure of merit (MF) is derived from the g-r noise to 1/f noise ratio normalized for frequency. High MF represents a low 1/f noise component.

$$MF = \frac{4\tau}{C_1 n}$$

where

τ = majority carrier lifetime

n = free carrier concentration

C_1 = 1/f noise constant

The figure of merit (MF) can be determined from the measured 1/f and g-r noise voltages if they are at least five times greater than Johnson noise. A Johnson noise plus amplifier noise correction can be made from the zero current noise figure.

$$MF = \frac{1}{\left[\frac{V_1^2 - V_o^2}{V_2^2 - V_o^2} - 1\right] f_1}$$

where,

V_1 = noise voltage in the 1/f noise frequency region

V_2 = noise voltage in the g-r noise frequency region

There is little difference between the row profiles. Etch No. 3 did not remove (Hg,Cd)Te at a detectable rate, hence, this row could not be completed. The slab is very inhomogeneous and prevents us from noting anything conclusive about this experiment. In Figure 12, detectors 7 and 8 show how lifetime and MF follow closely. C_1 is unchanged, but the 1/f noise is masked by a rising g-r noise plateau.

Passivation Coating - In the process of making devices for the dc field effect experiment, the effects of evaporated ZnS coating on the active area were investigated. The detector D* τ, MF, and C_1 were measured before and after coating, and no difference was detected. The coatings were 5 μm thick and an indium electrode was evaporated on the ZnS thus forming a parallel plate capacitor structure. The lack of change in D*, τ, MF, and C, assured us that the ZnS did not add surface states which could contribute to 1/f noise.

Initial Experimentation

Wedge Experiment - The object of this experiment was to determine the effect of thickness on 1/f noise. The slab is assumed to be uniform from left to right. The slab and substrate were mounted on a lapping plug at a slight angle by placing a thin strip of mylar under one corner of the substrate. The slab is processed in a wedge shape so that there is a thickness gradient from left to right.

Figure 13 is a cross-sectional view of the device. If the bulk resistance is much greater than the surface resistance, the device will show no resistance dependence on thickness;

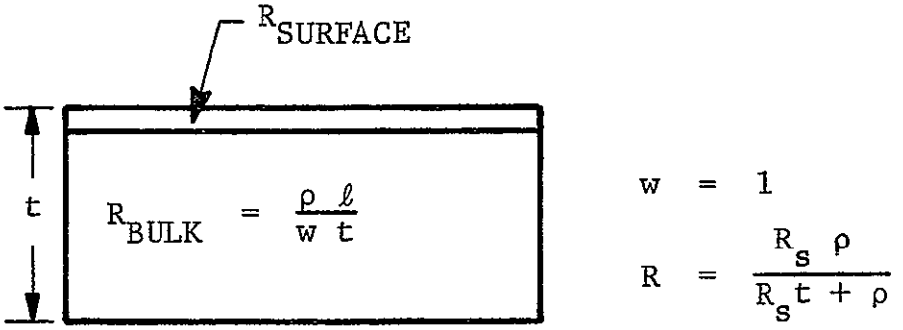

Figure 13 DEVICE CROSS-SECTION

the resistance will be entirely determined by the surface.

$$R = R_s$$

If the surface resistance is high then, $R = \rho/t$. When noise spectra are measured, a constant current generator is used.

$$V_c = i\,R$$

$$i = \text{constant}$$

$$\frac{dv}{dt} = i\,\frac{dR}{dt}$$

$$R = \frac{R_s\,\rho}{R_s t + \rho}$$

$$\frac{dR}{dt} = \rho^2\,\frac{\frac{dR_s}{dt} + R_s t\,\frac{d\rho}{dt}}{(R_s t + \rho)^2}$$

Case 1.

$$R = R_s \quad \text{or} \quad R_s \ll \rho/\tau$$

$$\frac{dR}{dt} = \frac{dR_s}{dt}$$

$$\frac{dv}{dt} = \frac{dR}{dt} \; i$$

Assuming the 1/f noise is not caused by contacts, this means the surface is the major cause of resistance fluctuations, and hence 1/f noise.

Case 2.

$$R = \rho/t \qquad\qquad R_s \gg \rho/t$$

$$\frac{dR}{dt} = \frac{1}{t} \frac{d\rho}{dt}$$

This shows that the resistance and noise voltage fluctuations will both be thickness dependent.

Table IV summarizes the data for this experiment. The resistance seems to be constant over a wide range and independent of thickness suggesting that it is surface conductivity dominated. However, this is in direct contradiction to previous wedge experiments performed at HRC on (Hg,Cd)Te which proved that it is bulk conductivity dominated. It is suspected that the material inhomogeneity was the cause of this different result.

TABLE IV
WEDGE EXPERIMENT

Slab 129 Device	t (μm)	R (Ω)	MF
B6	32.5	115	2.27×10^{-5}
C6	25	137	2.5×10^{-6}
A6	20	137	1.17×10^{-5}
D6	15	137	8.5×10^{-6}

dc Field Effect - In the dc field effect experiment samples of (Hg,Cd)Te were covered with a thin layer of dielectric on which was placed a metal electrode to complete a capacitor arrangement, (Figure 14). A voltage was applied to the metal electrode giving an electric field perpendicular to the surface of the (Hg,Cd)Te and thereby changing the surface potential by drawing electrons to the surface. Changes in the surface potential can be monitored by noticing differences in the conductivity of the sample. These surface potential changes would then be correlated with a change in 1/f noise voltage. In the dc field effect experiment we would expect to see changes in the sample conductivity which were related to the long relaxation times of the slow surface states.

This experiment was first performed with a 25 μm thick (Hg,Cd)Te sample with a 50 μm thick dielectric of mylar and an indium top metal electrode. When the metal top electrode was raised to 200

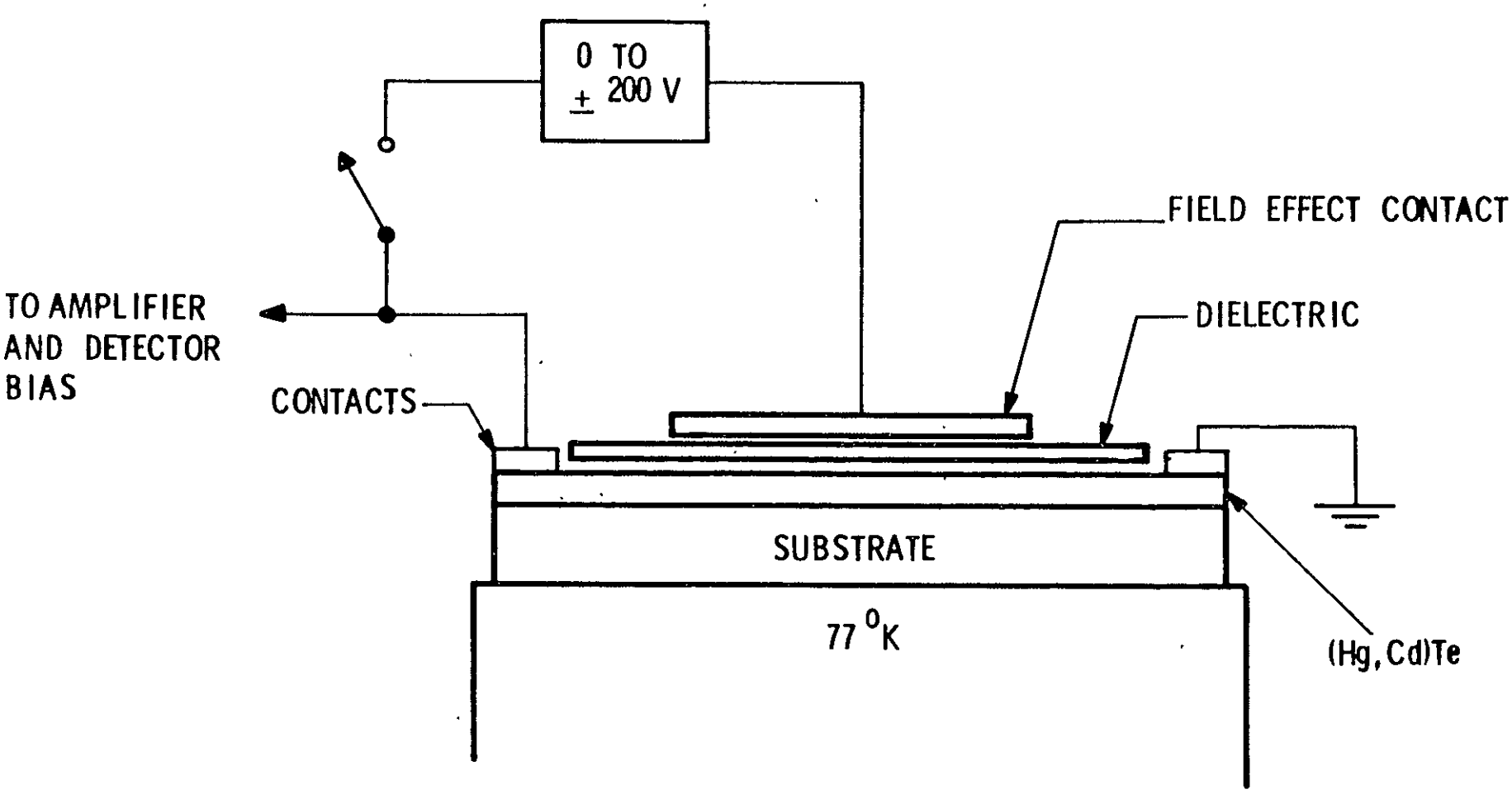

Figure 14 DC FIELD EFFECT EXPERIMENT

volts, no change in conductivity or 1/f noise voltage was noticed. To increase the transverse field, the mylar was replaced with a 5 μm thick evaporated ZnS dielectric. Although fields as high as 4×10^5 V/cm were attained with the ZnS dielectric, still no change in conductivity or 1/f noise could be noted. The results of this experiment did not confirm the existence of slow surface states in 15 micron (Hg,Cd)Te nor their relation to 1/f noise.

Magnetic Field Effect - In an attempt to change the surface of (Hg,Cd)Te samples, the following qualitative experiment was performed. A magnetic field was placed parallel to the surface of the sample, perpendicular to the bias current. Holes and electrons are thus driven to one of the surfaces depending on the field direction as shown in Figure 15.

Noise voltages vs bias current was plotted as a function of magnetic field in Figure 16 and it was found that the 1/f noise increased by a factor of 2, larger than that expected from magnetoresistive effects. The fact that driving carriers to the surface of the sample affects 1/f noise voltage suggests a possible relationship between the surface of 15 μm (Hg,Cd)Te and 1/f noise. Montgomery[8] and Suhl[24] explained the magnetic field effect in terms of the change in lifetime of carriers due to the fact that the recombination of carriers occurs mainly near the surface and is proportional to their density there. However, the theory does not explain the source of the conductivity modulations, only the effect of driving the current to the surface.

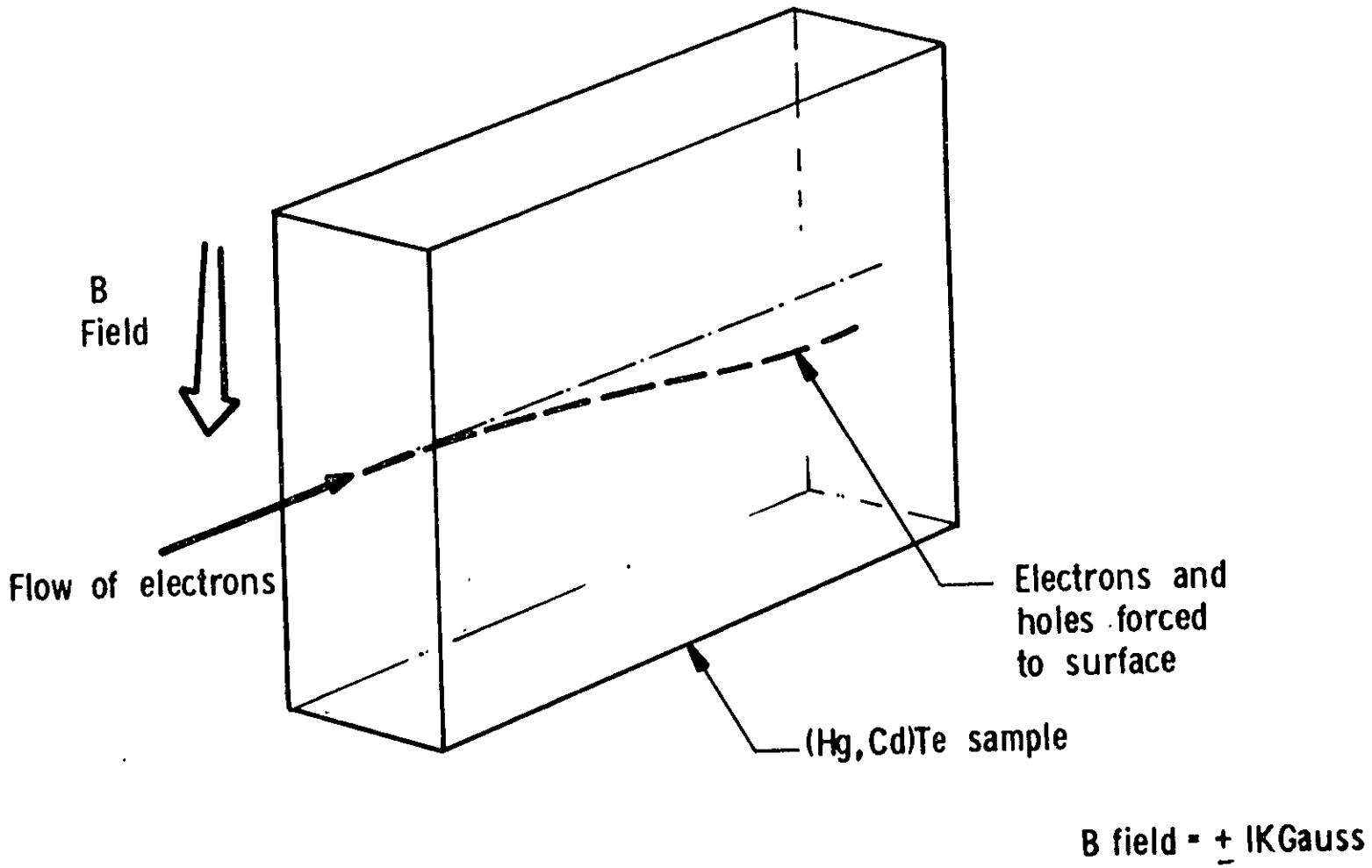

Figure 15 MAGNETIC FIELD EFFECT EXPERIMENT

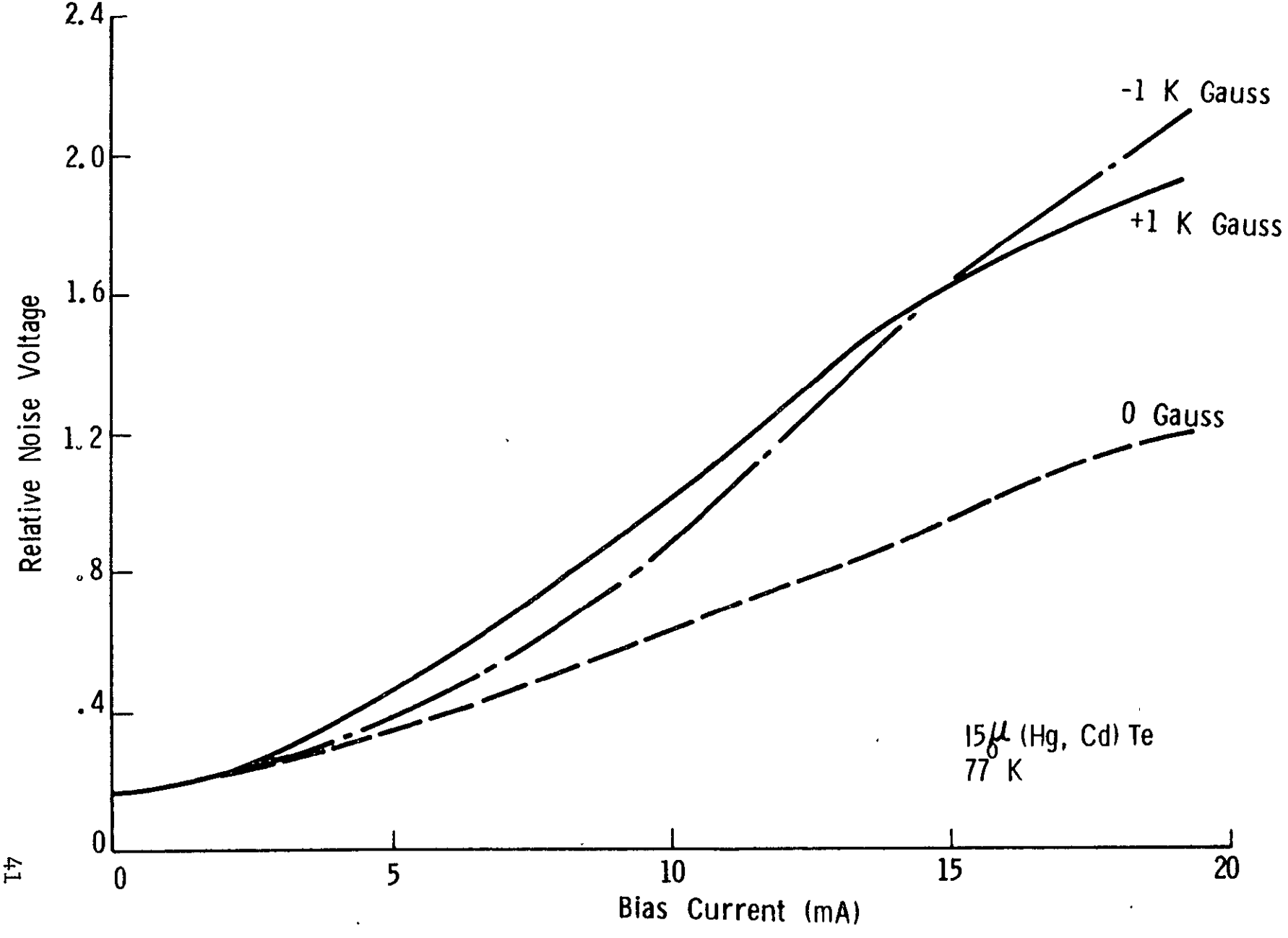

Figure 16 MAGNETIC FIELD EXPERIMENT - NOISE VOLTAGE (3 kc) VS BIAS CURRENT

Later Experimentation

Four Contact Experiment - To find the contributions of the contacts to the 1/f noise, we have made use of the four-contact experiment. A four-contact sample (see Figure 17) is used which has two current injecting contacts at the ends and two equally spaced voltage sidearm probes. This gives us three distinct segments, two end segments which contain bias contacts and one internal segment which only contains bulk material.

To insure the independence of the noise in each segment, two constraints must be satisfied. First a constant current generator insures that the noise voltage between probes is dependent only upon resistance and carrier fluctuations between the two probes. Secondly, the life path, or distance carriers travel before recombining, ($\ell = \mu\tau E$ where μ = mobility, τ = carrier lifetime, and E = bias field) is made small to insure that carrier modulations in one segment are not swept into an adjacent segment and measured as noise in that region. Thus the noise voltage of each segment is independent of adjacent segments. If the end contacts are a source of 1/f noise, then we would expect V_{12} and V_{34} to be relatively larger than V_{23}, while if the source of 1/f noise is the surface or bulk, we could expect all segments (including the internal segment V_{23}) to be dependent upon some material parameter such as sample resistance.

Figures 18, 19, and 20 show the results of this experiment where we have given the noise voltage at 100 Hz in relative units

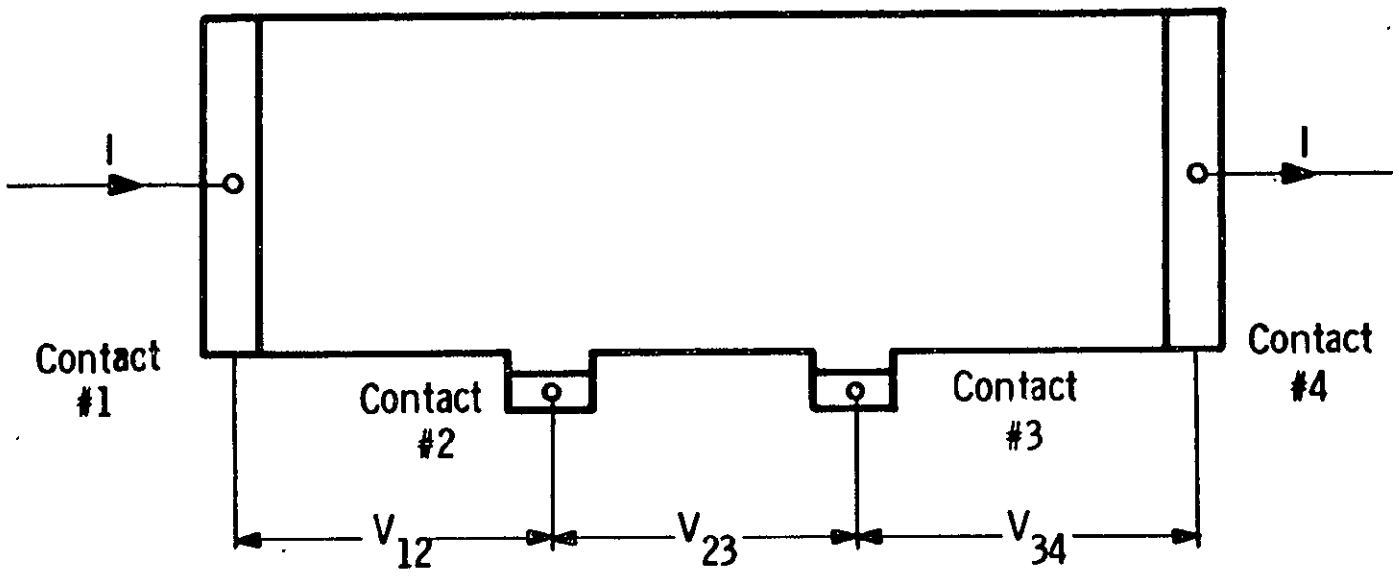

Figure 17 FOUR CONTACT SAMPLE

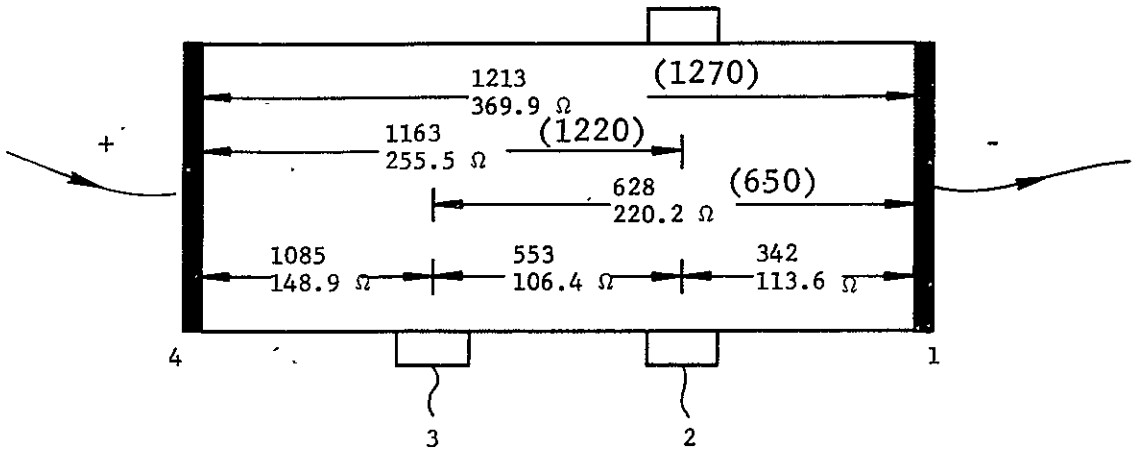

a) Forward Bias

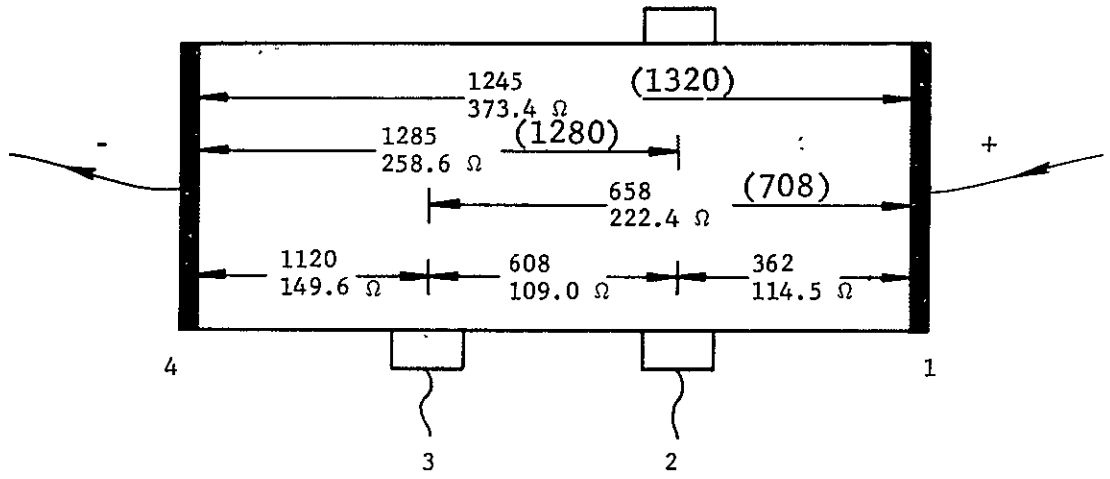

b) Reverse Bias

Figure 18 RELATIVE 1/f NOISE VOLTAGE AT 100 Hz AND RESISTANCE IN 4 CONTACT EXPERIMENT (SAMPLE NO. 2 (SOLDERED END CONTACTS))

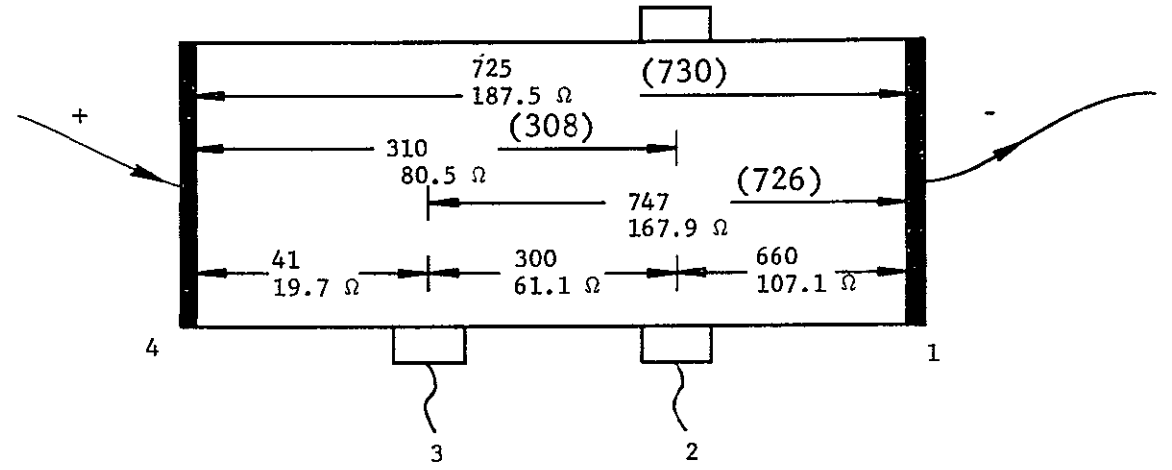

a) Forward Bias

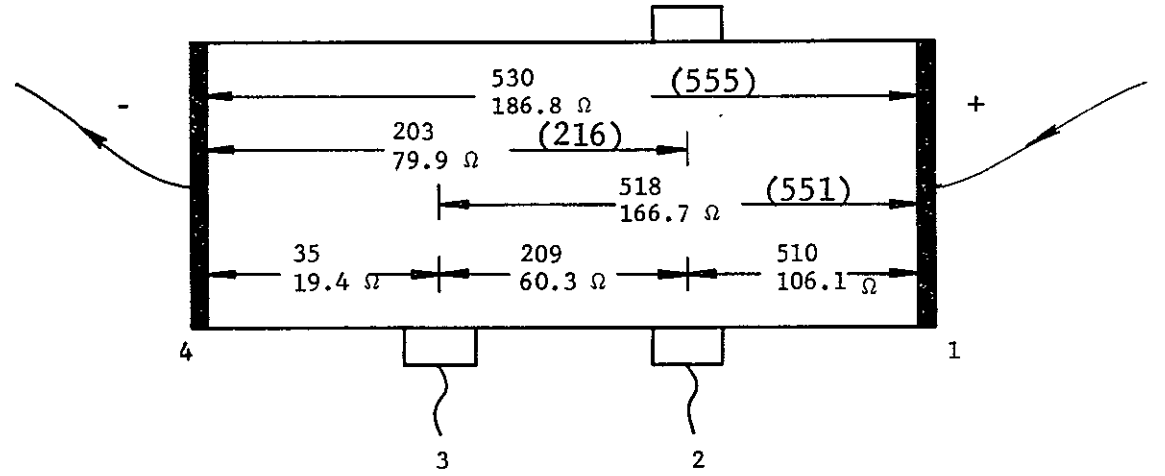

b) Reverse Bias

Figure19 RELATIVE 1/f NOISE VOLTAGE AT 100 Hz AND RESISTANCE IN 4 CONTACT EXPERIMENT (SAMPLE NO. 3 (TC BONDED CONTACTS))

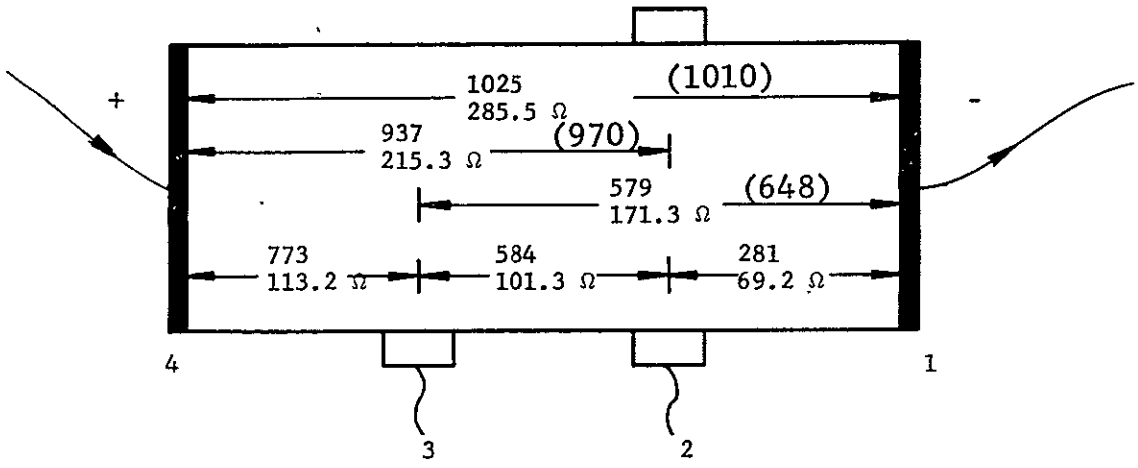

a) Forward Bias

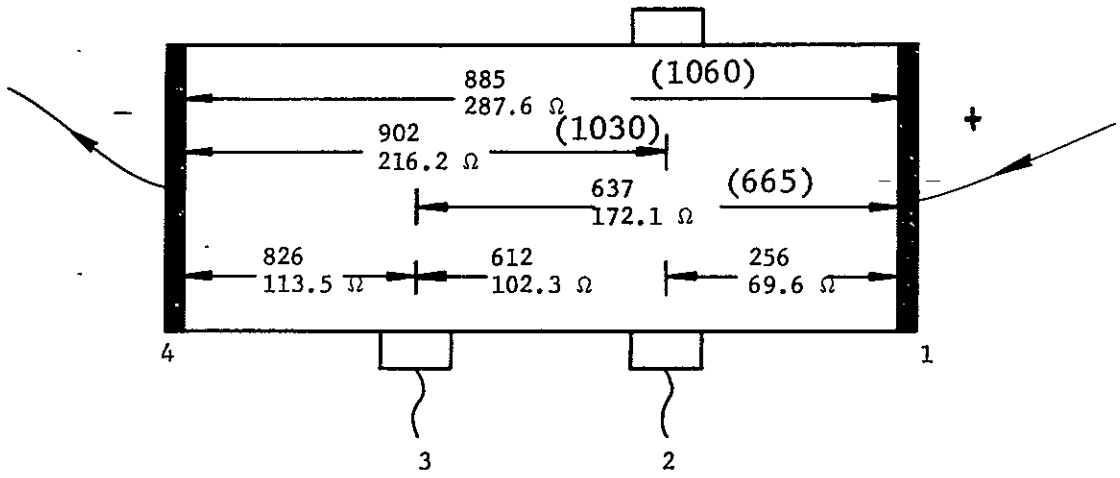

b) Reverse Bias

Figure 20 RELATIVE 1/f NOISE VOLTAGE AT 100 Hz AND RESISTANCE IN 4 CONTACT EXPERIMENT (SAMPLE NO. 4 (TC BONDED CONTACTS))

on top and resistance along the sample below for each of the possible combinations of segments. Sample number 2 had soldered contacts while samples 3 and 4 were TC bonded on indium pads.

The noise voltage of multiple segments (i.e., 2 and 4, 3 and 1, 4 and 1) are close to the calculated vectorial sum of the noise voltages in the single segments. We have included the calculated sums in parenthesis in Figures 18 to 20. Only sample number 3 exhibited a marked change ($\approx$ 35%) in 1/f noise voltage when the bias was reversed, however, the increase was uniform throughout the segment measurements and the noise still added vectorially.

Noise voltages V_{12}, V_{23}, and V_{34} at 100 Hz for all samples were plotted vs resistance (Figure 21) in the single segments which are of uniform length and cross-sectional area. Not only did the internal contacts (noted by a circle) and external contacts of each sample follow the same resistance dependence, but that all three samples followed the same resistance dependence regardless of contact type. In all cases, the 1/f noise voltage was proportional to resistance to the 1.7 power. This suggests that 1/f noise voltage is independent of the contacts and is within the bulk or surface of the material.

Figure 22 shows full noise spectra for all single segments and the full length of four contact sample number 4. We see that although the voltage level varied with respect to single segment resistance to the 2.5 power, the slope α showed little to no change. This suggests that only the magnitude and not the nature of the 1/f noise changes with resistivity.

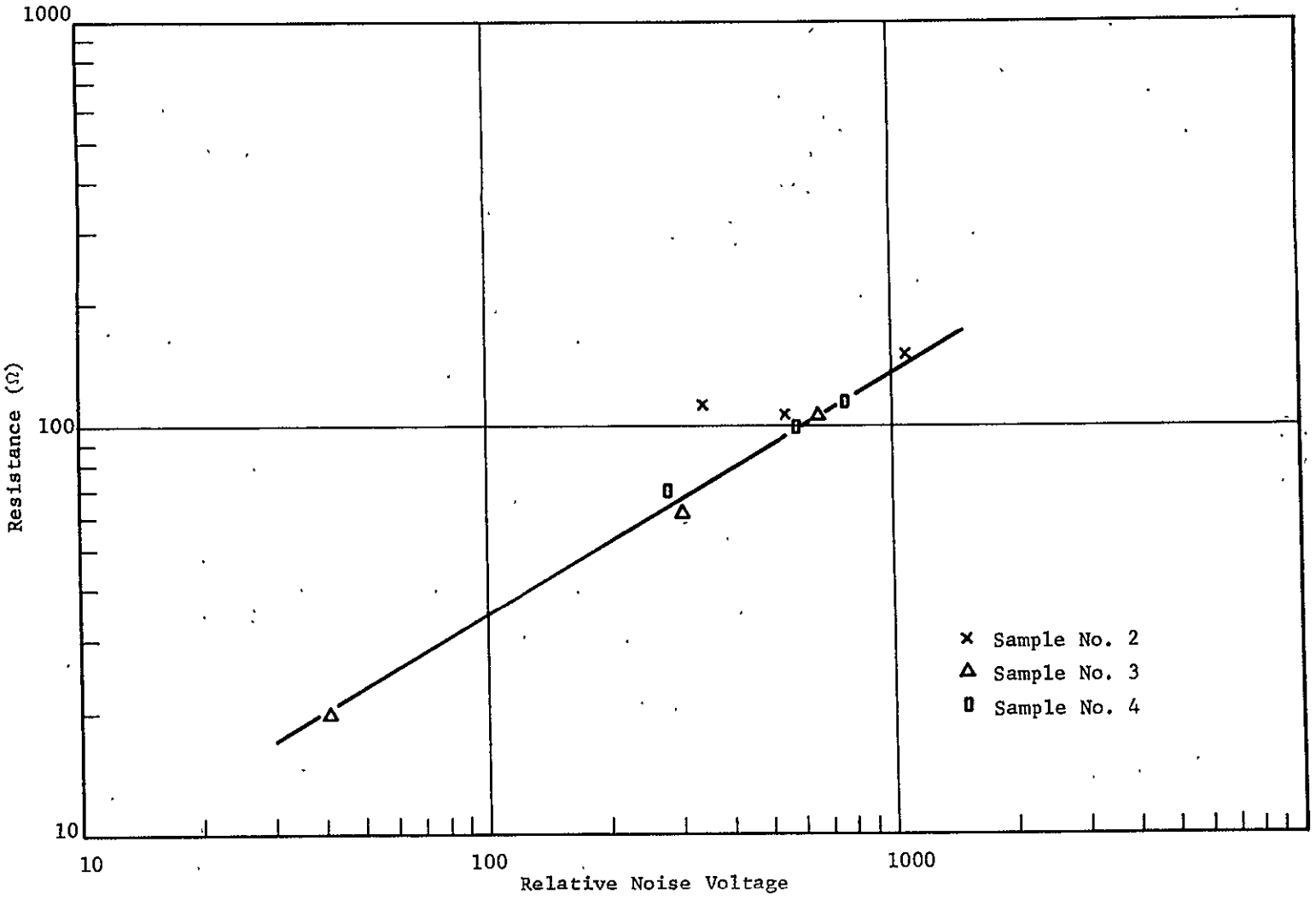

Figure 21 RELATIVE NOISE VOLTAGE VS RESISTANCE IN SINGLE SEGMENT OF 4 CONTACT SAMPLES

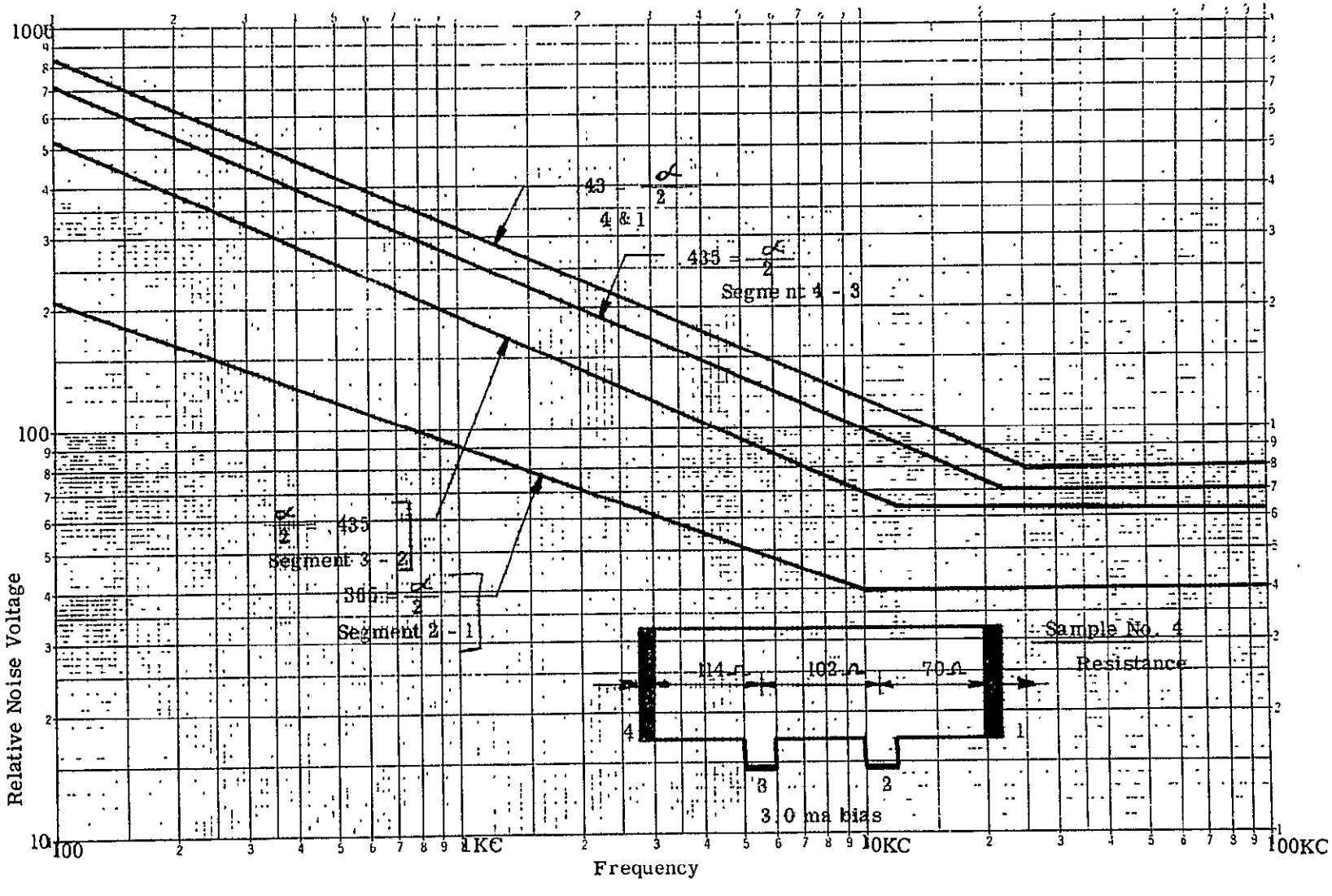

Figure 22 FULL NOISE SPECTRA FOR ALL SINGLE SEGMENTS AND THE FULL LENGTH OF SAMPLE 4

Background Dependence of 1/f Noise - A study of the effect of background temperature on 1/f was performed. A special dewar was prepared which had no window and allowed the detector a 180-degree FOV into a black background. The detector was always cooled to 77 °K while data was taken for a background of 300 °K and then 77 °K. Data was taken for three high performance detectors and one Hall sample whose resistance at 77 °K and 295 °K backgrounds are given in Table V.

TABLE V
HALL SAMPLE DATA

Slab	Sample	Resistance 295° Background	Resistance 77° Background
144	B5	100	151
144	D5	114	145
149	D9	37.8	37.0
127	HS4	289.9	494.7

The resistance increased by 50% for sample B5. The noise spectra for each detector at 77 °K background and 295 °K background are given in Figures 23 to 26. In each case, the bias current was kept constant in the experiment despite the increase in detector resistance. We see that only sample D5 of slab 144 showed any real decrease in 1/f noise level although the increased resistance at lower background temperature for all the samples indicates an effective lowering of the 1/f noise coefficient C_1 since (see P.W. Kruse et al, Elements of IR Technology[13], p. 255)

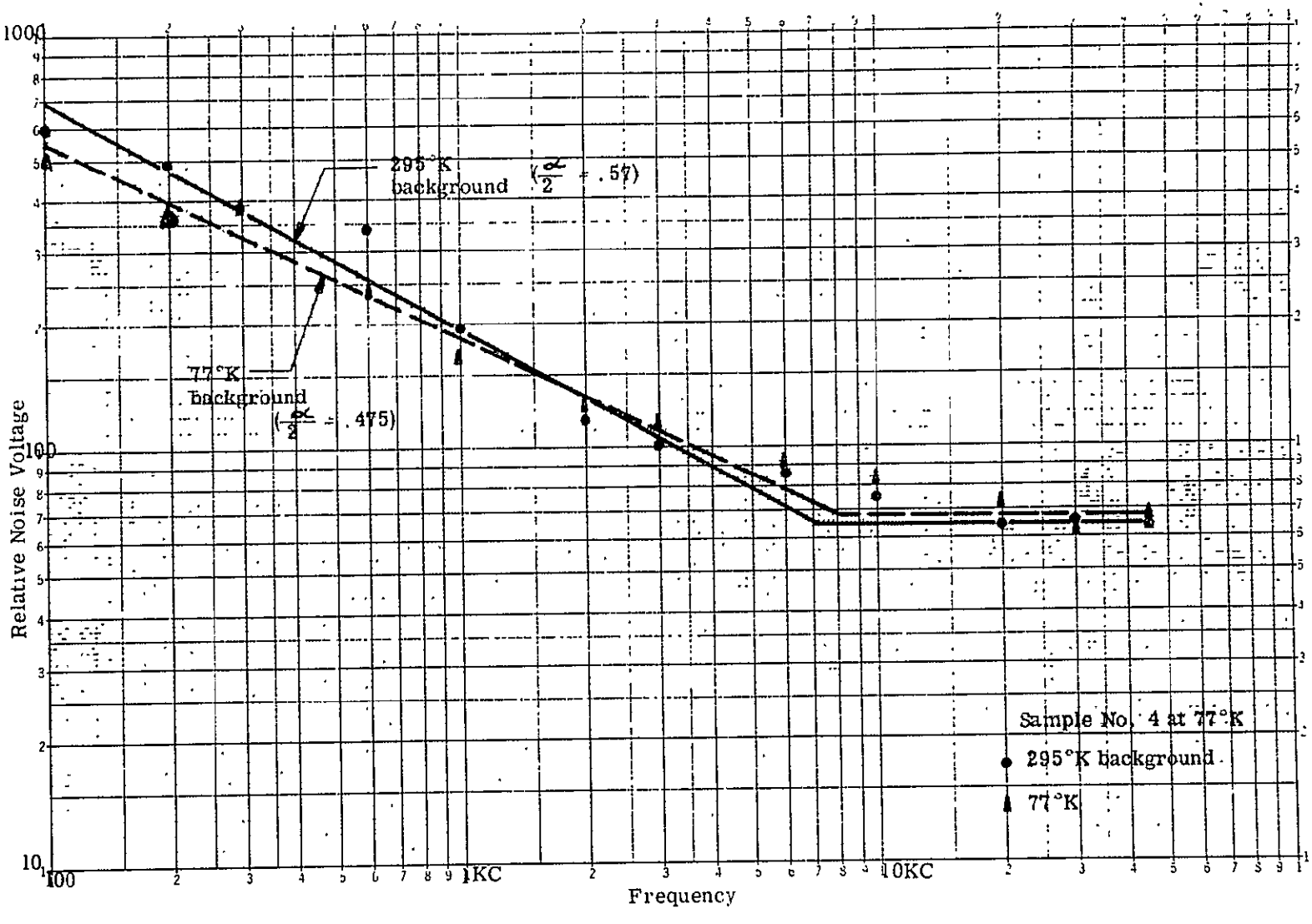

Figure 23 NOISE SPECTRA FOR SAMPLE NO. 4

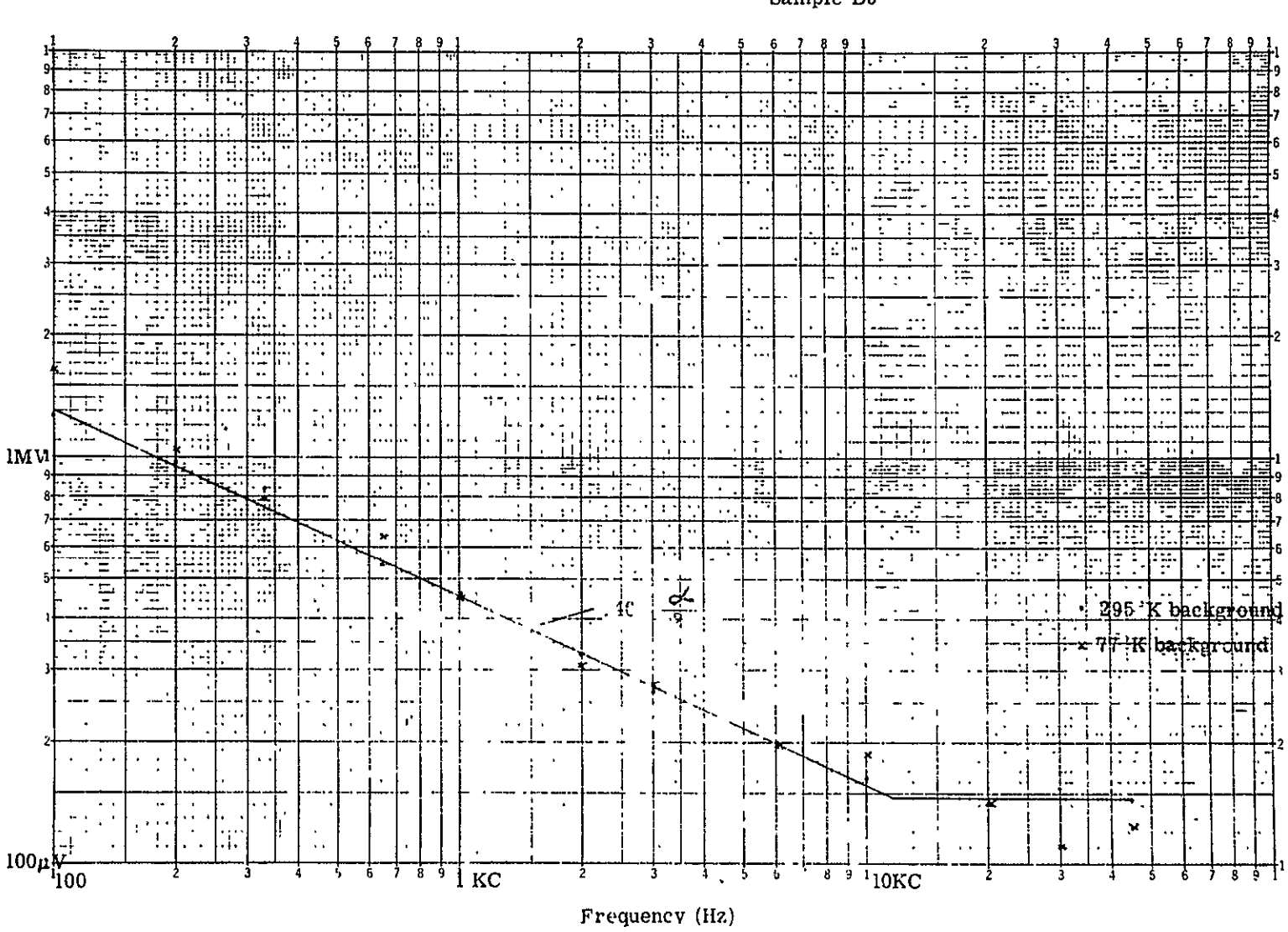

Figure 24 NOISE SPECTRA FOR SAMPLE NO. B5

Sample D6

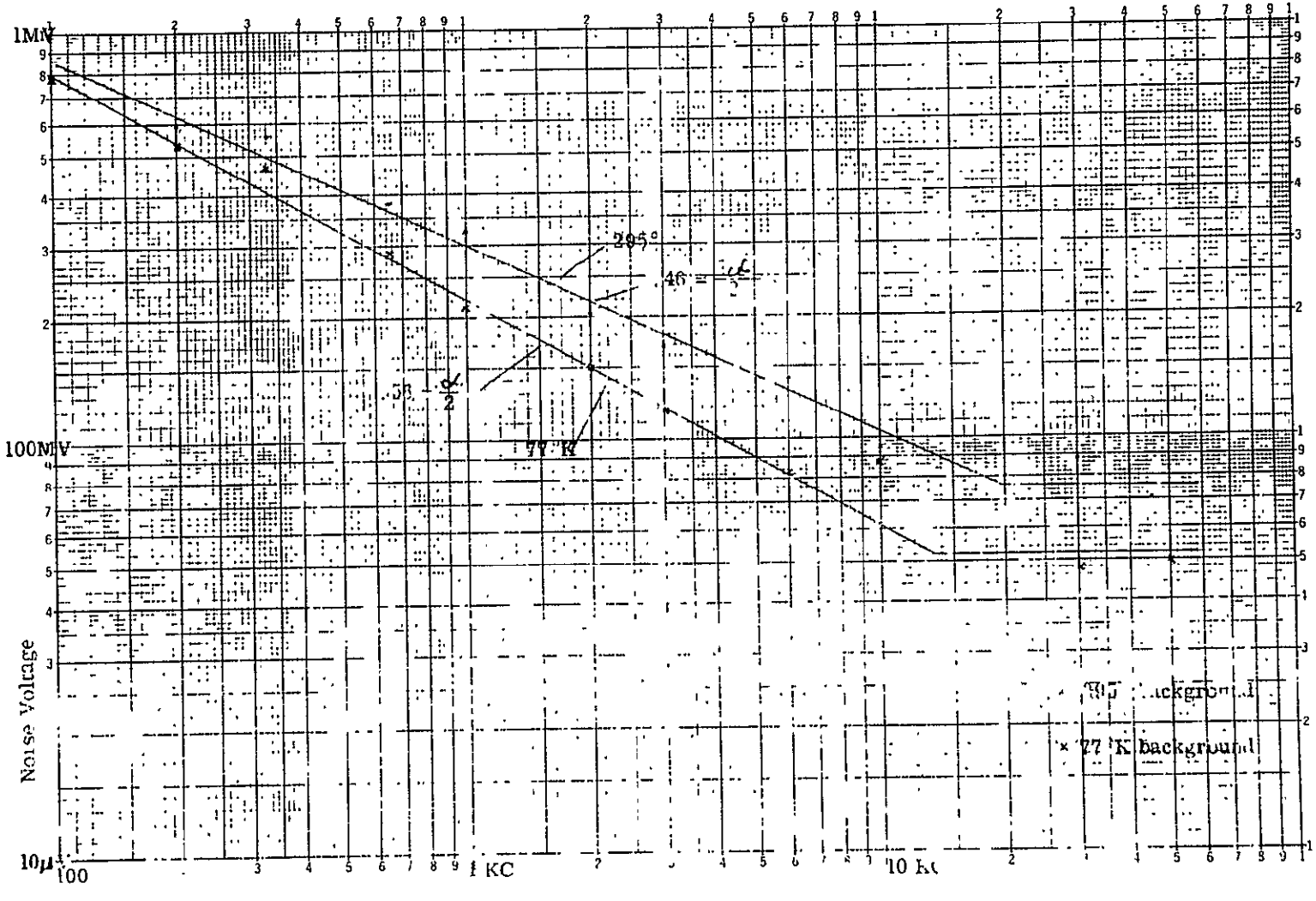

Figure 25 NOISE SPECTRA FOR SAMPLE NO. D6

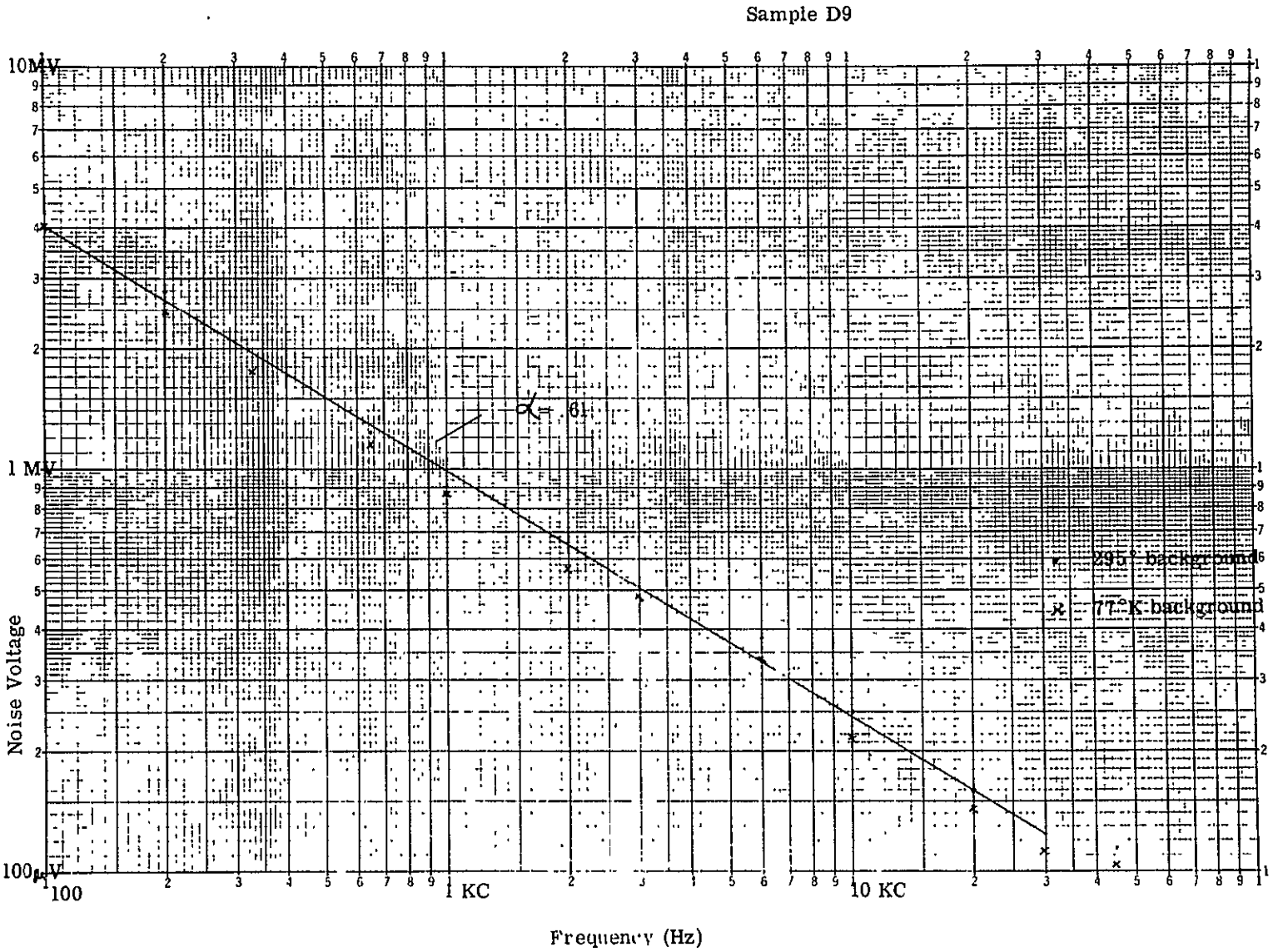

Figure 26 NOISE SPECTRA FOR SAMPLE NO. D9

$$V_{1/f} = \frac{C_1^{1/2} \rho I \ell^{1/2} (\Delta f)^{1/2}}{f^{1/2} (A)^{3/2}}$$

Any increase in ρ at constant bias without a corresponding increase in $V_{1/f}$ constitutes an effective lowering of the 1/f coefficient C_1.

Sample D5 showed a slight increase in slope from 0.46 to 0.56 as the background temperature was lowered. However, the effect on the 1/f knee was minimal since the g-r level also lowered slightly. τ the lifetime was measured and found to remain constant within experimental error at 100 nanoseconds.

B.L. Musicant has reported in private communication that cold aperturing has decreased the 1/f knee in one of his samples from 2400 to 360 cycles while increasing the lifetime from only 260 to 430 nanoseconds. The resistance in his sample increased from 16 to 24 Ω. Such background dependent data suggests that cold aperturing could at worst effectively lower C_1 and bias power consumption by increasing device resistance.

Relationship of Material Parameters and 1/f Noise - H. I. Andrews has plotted μ vs n from available Hall data for many samples with peak wavelength response between 8-14 μm. He has found a relation between μ and n which suggests that μ and n are not independent parameters (Figure 27). In Figure 28 μ vs n is plotted for material used in our 15 μm 1/f study. (We have also included

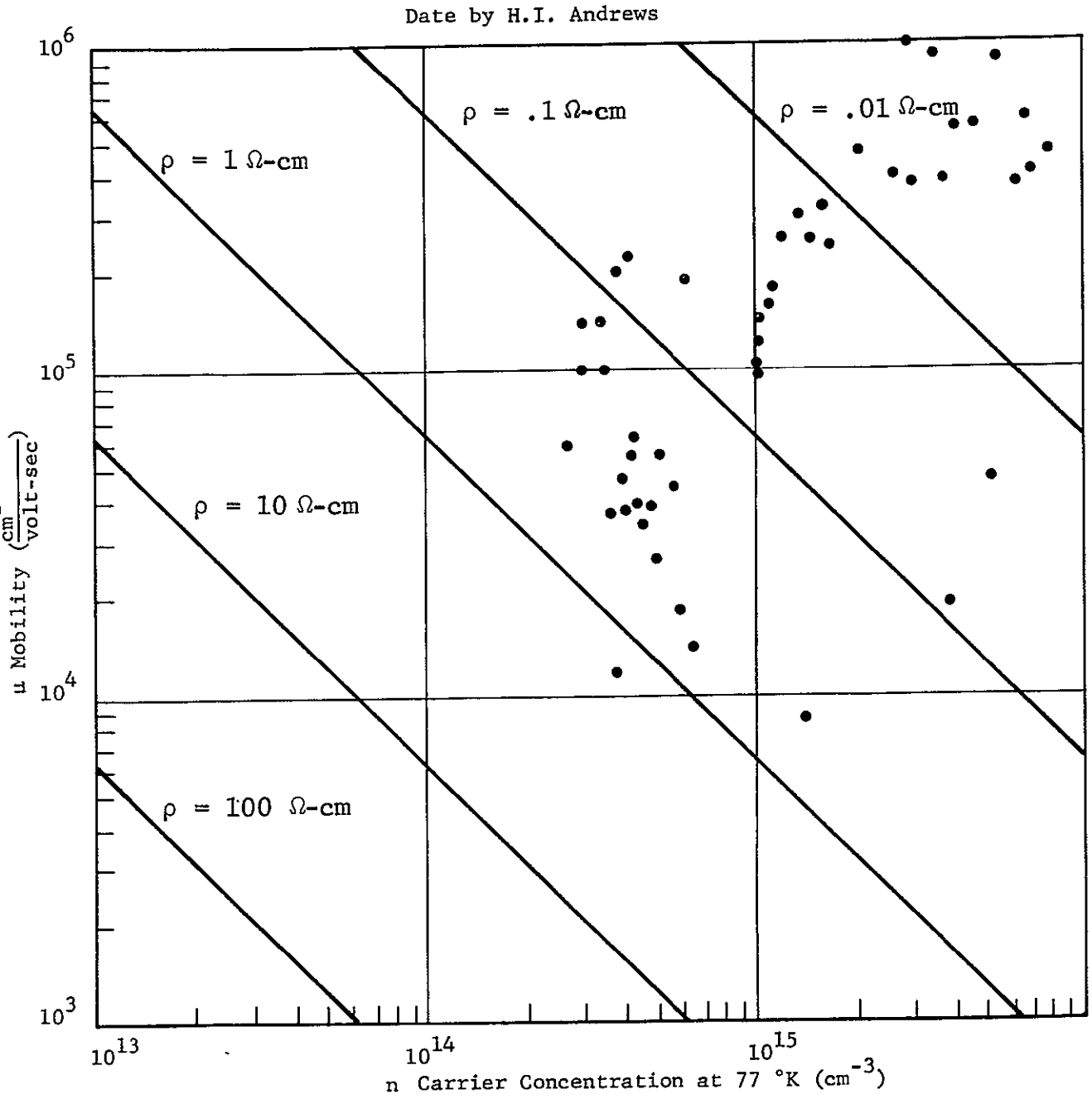

Figure 27 CARRIER CONCENTRATION VS μ MOBILITY

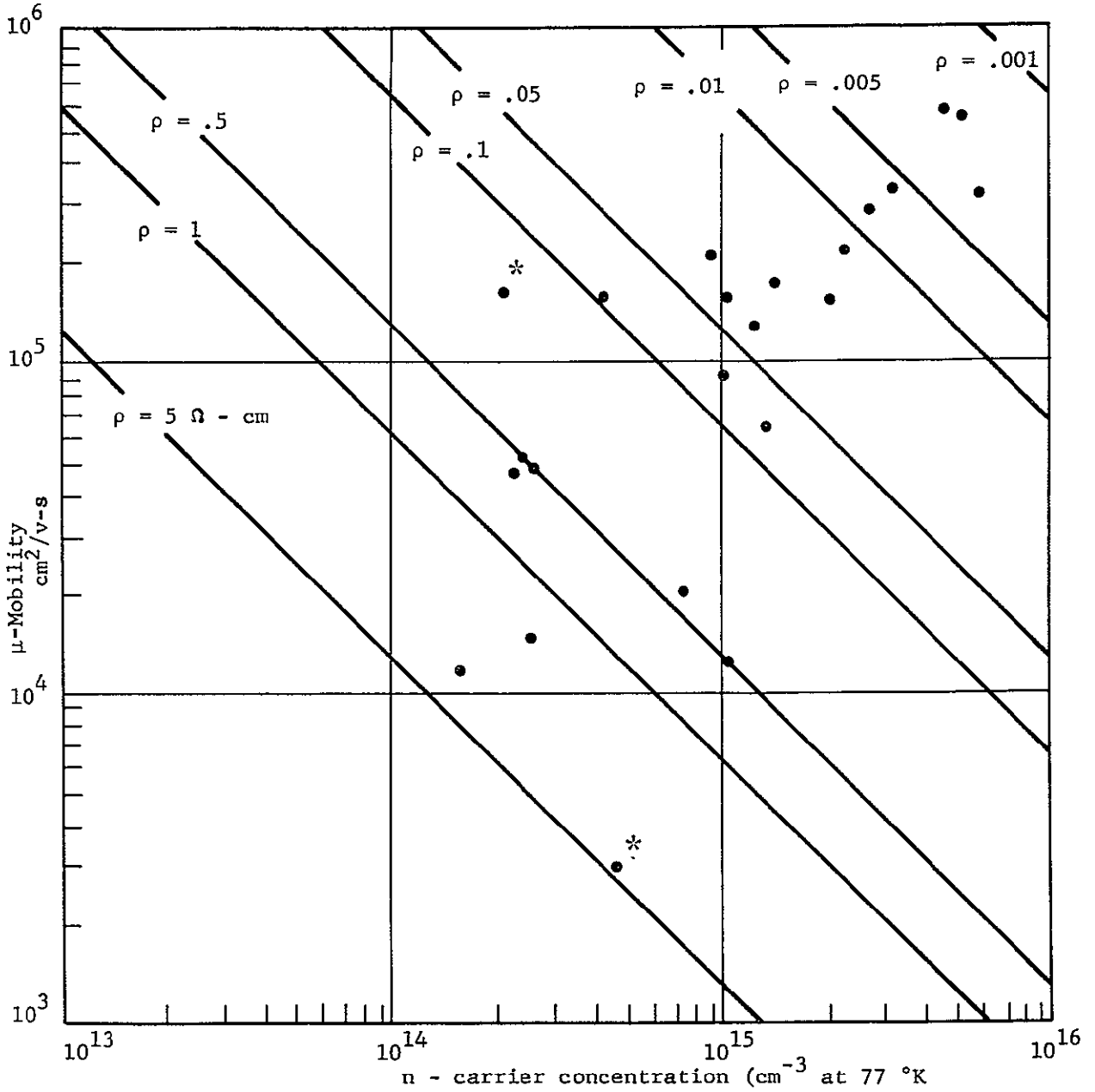

* Hall data
partially p-type

Figure 28 μ VS n

some available data on other long wavelength slabs). Essentially, the same relationship exists between μ and n although not as dramatic due to the smaller number of samples available. Lines of constant resistivity are included on both graphs. We see that up until about 0.5 ohm-cm, μ and n exhibit an almost linear relationship, that is, as the carrier concentration decreases, the charge mobility decreases also. In Andrews' data deviations from this linear relationship are seen to occur after 0.5 ohms/cm. The data points follow the 0.5 ohm-cm line so that the mobility still decreases while the carrier concentration increases. This is a very interesting effect in that previous data by A.N. Kohn and L.C. White has shown that the 1/f noise coefficient C_1 is proportional to $\rho^{5/2}$ until $\rho \approx 0.4$ ohm-cm. When $\rho > 0.4$ ohm-cm the 1/f noise coefficient cannot be correlated with resistivity. We suspect that these two phenomena are related.

Andrews has also found a correlation between the Hall data points and their position in the slab. We have seen somewhat the same correlation in that high n, high μ material usually comes from the Hg rich region at the bottom of the slab. Hall data taken from samples progressively higher in the slab follow the curve of Figure 27 in that as n is decreased μ is also lowered until the turn around point of ρ = 0.5 ohm-cm. The fact that resistance of detectors increases as we go up in the slab has generally been found to be true for our samples and is expected due to the fact that x the mole fraction of CdTe in the material, and along with it the bandgap and λ_{co} of the sample, is changing. However, samples have been found which have the same

λ_{co}, thickness, and aspect ratio and yet the resistance differs by a factor of 10. Compare for example the two detectors.

Slab	Element	Thickness	Aspect Ratio	λ_{peak}	λ_{co}	Resistance
127	B8	25 μm	1	14.5 μm	16.5 μm	90.5 Ω
S1	C8	25 μm	1	14 μm	16 μm	8 Ω (no 1/f at 1kc)

This seems to be an indication of the fact that some mechanism increases the resistance of the samples. The same mechanism which increases this resistivity, could also be the source of the 1/f noise and thus explain the resistivity dependence of C_1. Since theories to explain this increased resistivity with its associated change in material parameters are possible, including segregation of material impurities, it is of prime importance to ascertain the nature of resistivity in (Hg,Cd)Te and the relationship of material parameters as a means for understanding and reducing 1/f noise.

High ρ Study

As discussed in a previous section, 1/f noise in some high resistance samples was studied. The samples used in this study consisted of detectors and Hall samples and are listed in Table VI along with their resistances, sizes, and wavelength. Included in this study were two Hall samples from slab 152 and detectors fabricated from the row adjacent to the Hall samples (row A). Two other samples of interest were studied at the same time. These are two Hall samples which had undergone the E anneal after the normal growth sequence. These samples represented the only major excursions from the linear relationship between μ and n seen in Figure 28.

TABLE VI
HIGH RESISTANCE SAMPLES

Slab	Sample	+Resistance(Ω)	-Resistance	Bias(mA)	λ_{co}(μm)
144	B5	100	133	0.8	> 14.5
152	A13	55.7	50.7	2.5	10
	A12	356	306	0.5	11
	A11	239	238	0.5	11
	A10	474	538	0.4	11
	A9	334	538	0.3	11.5
	A8	328	278	0.5	13
	HS5	1217	1182	2.5	
	HS4	1218	1092	2.5	
$125_{E anneal}$		731	735	2.5	
146		958	961	2.5	
149	D9	38	38	6	11
All data at 77 °K					

Noise spectra were taken for all samples at their optimum bias for forward and reverse bias conditions. Figures 29 to 36 are the noise spectra for detectors while 37 to 40 are those of the Hall samples where 39 and 40 are the E anneal spectra. Although the noise level for all detectors is high as expected from their high resistivity, only one sample (A12) showed a significant change in 1/f noise level (a factor of 2) for different bias direction, while all others were within a factor of 1.5. The slope of the curves or the value for $\alpha/2$ ranged from 0.38 to 0.77 with the majority of the

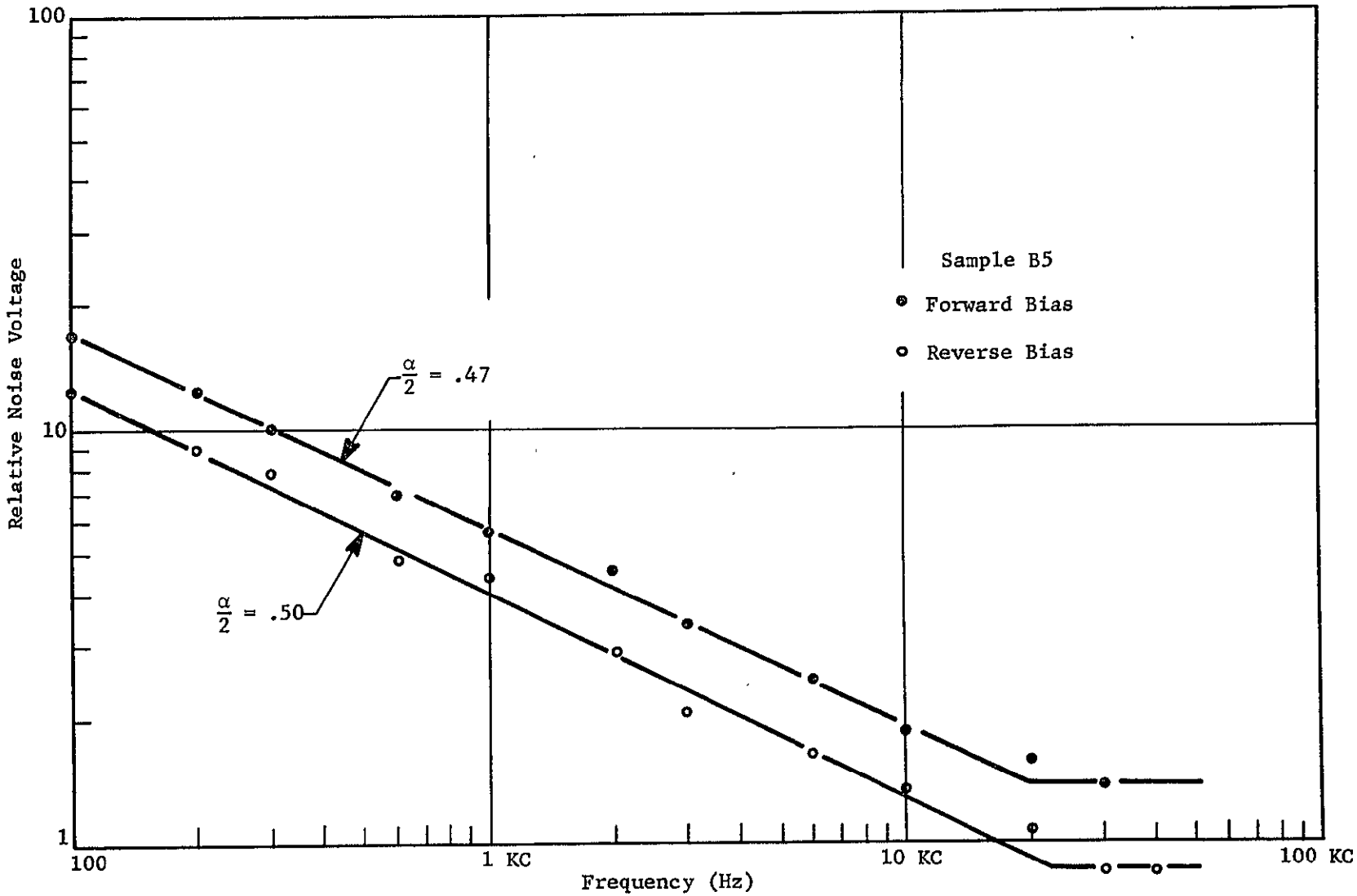

Figure 29 SAMPLE B5 DATA

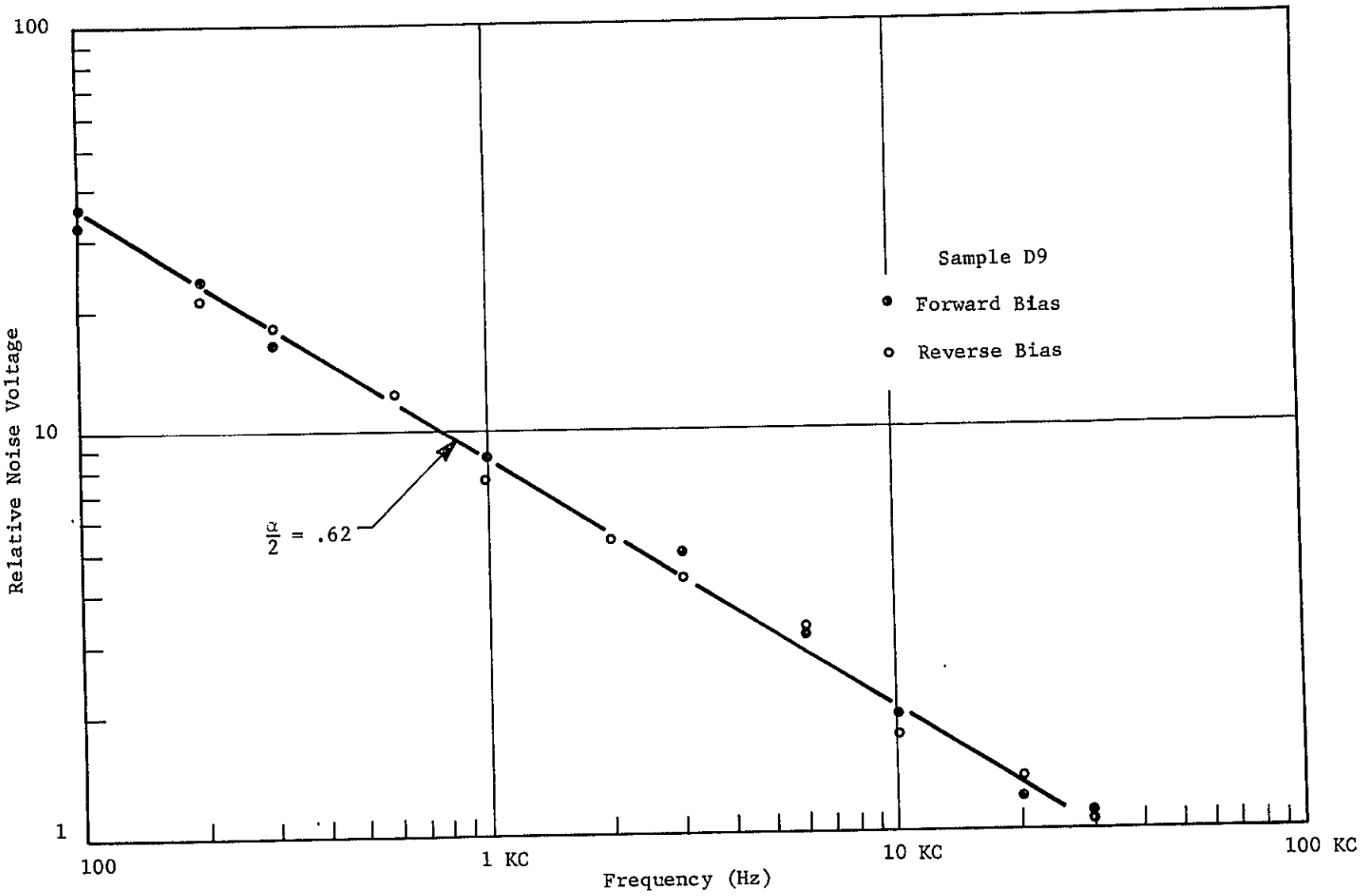

Figure 30 SAMPLE D9 DATA

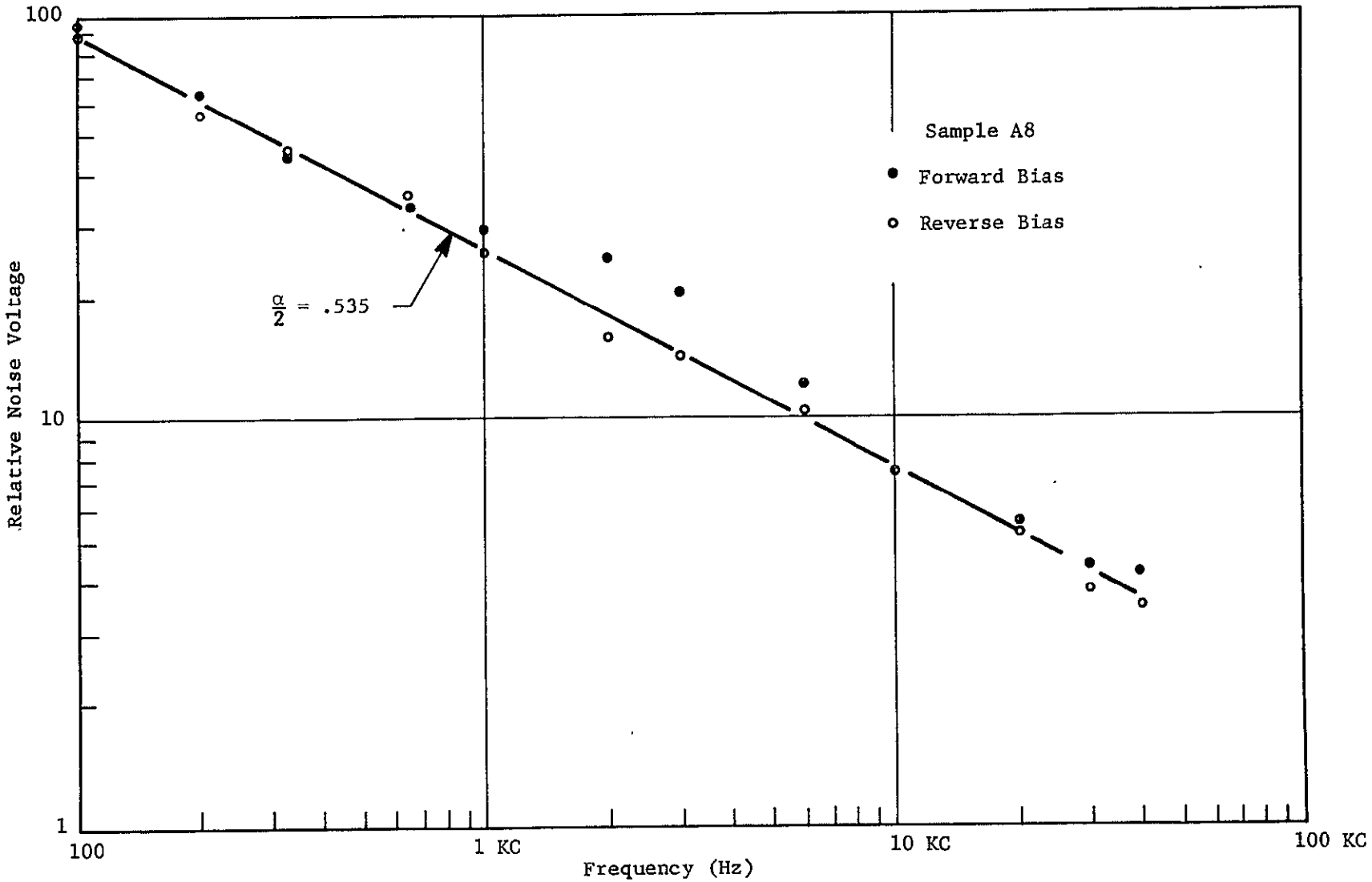

Figure 31 SAMPLE A8 DATA

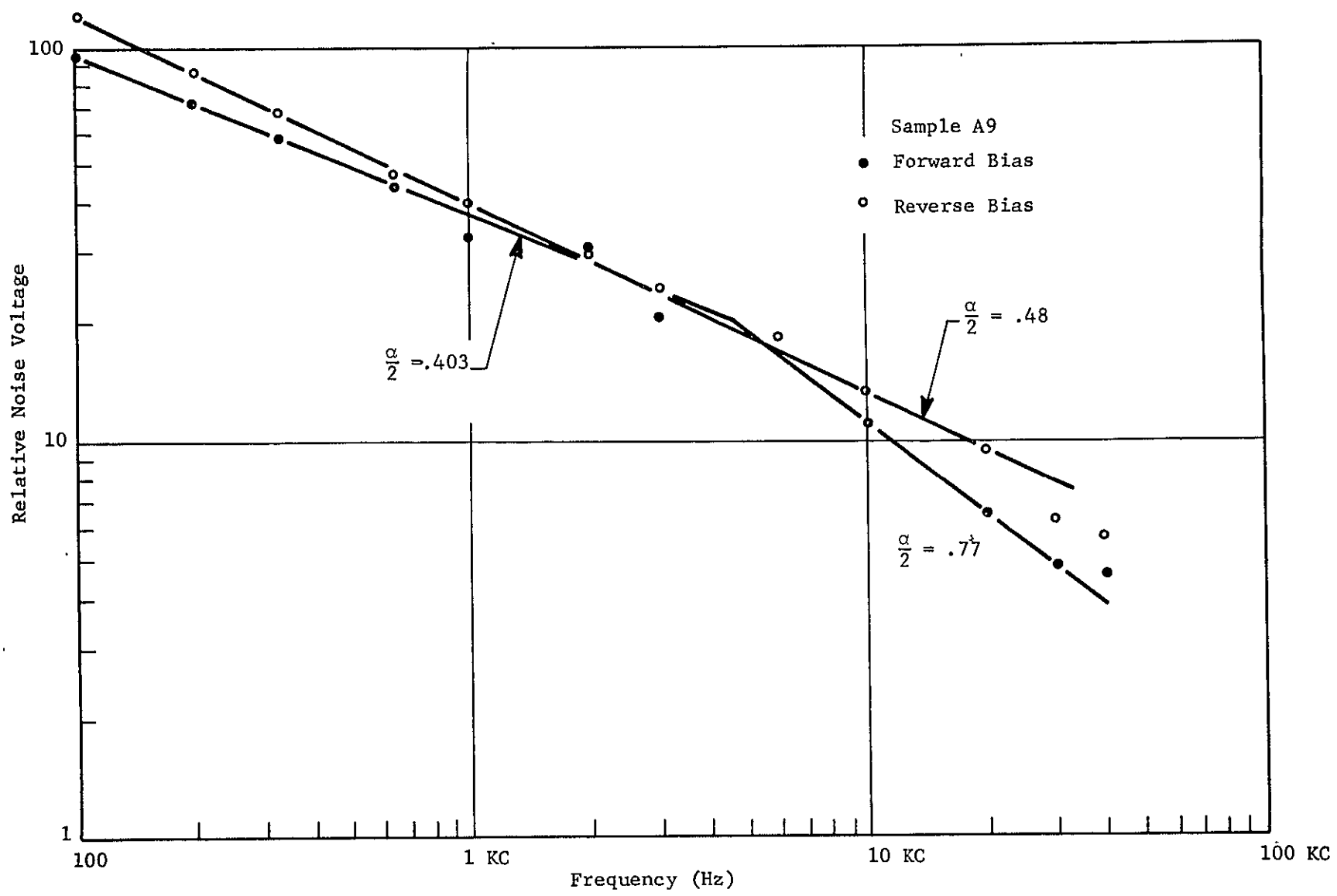

Figure 32 SAMPLE A9 DATA

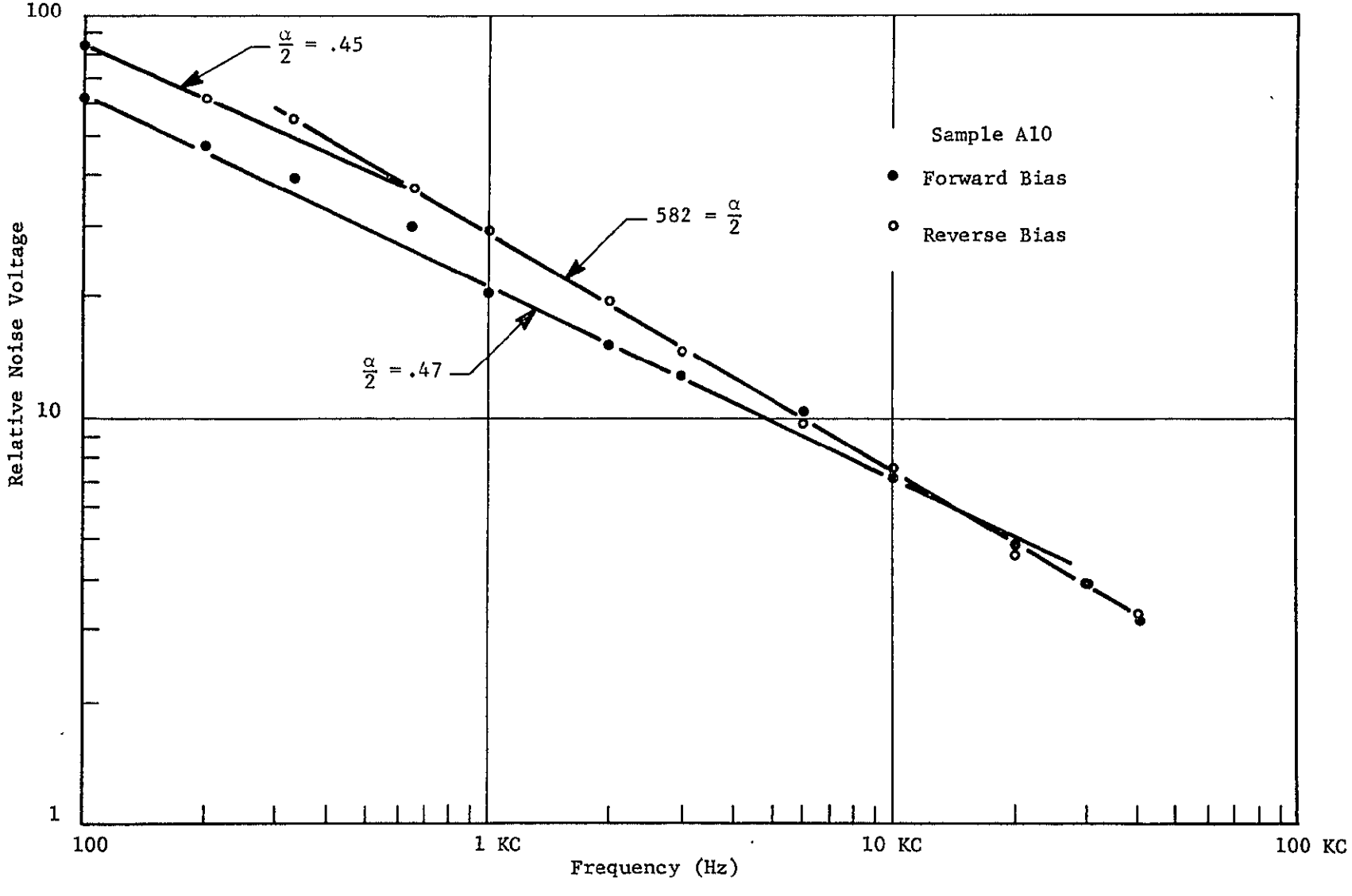

Figure 33 SAMPLE A10 DATA

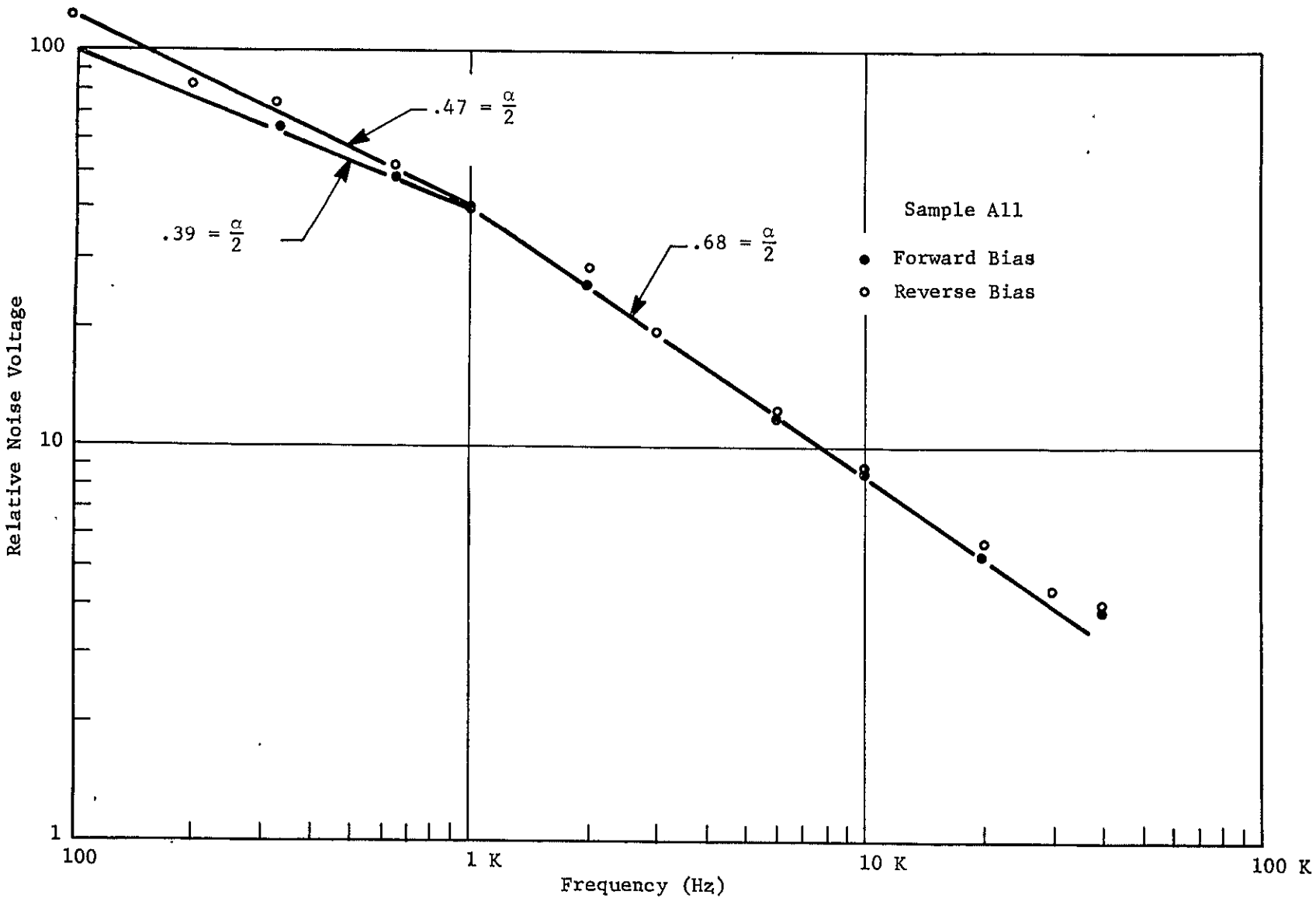

Figure 34 SAMPLE A11 DATA

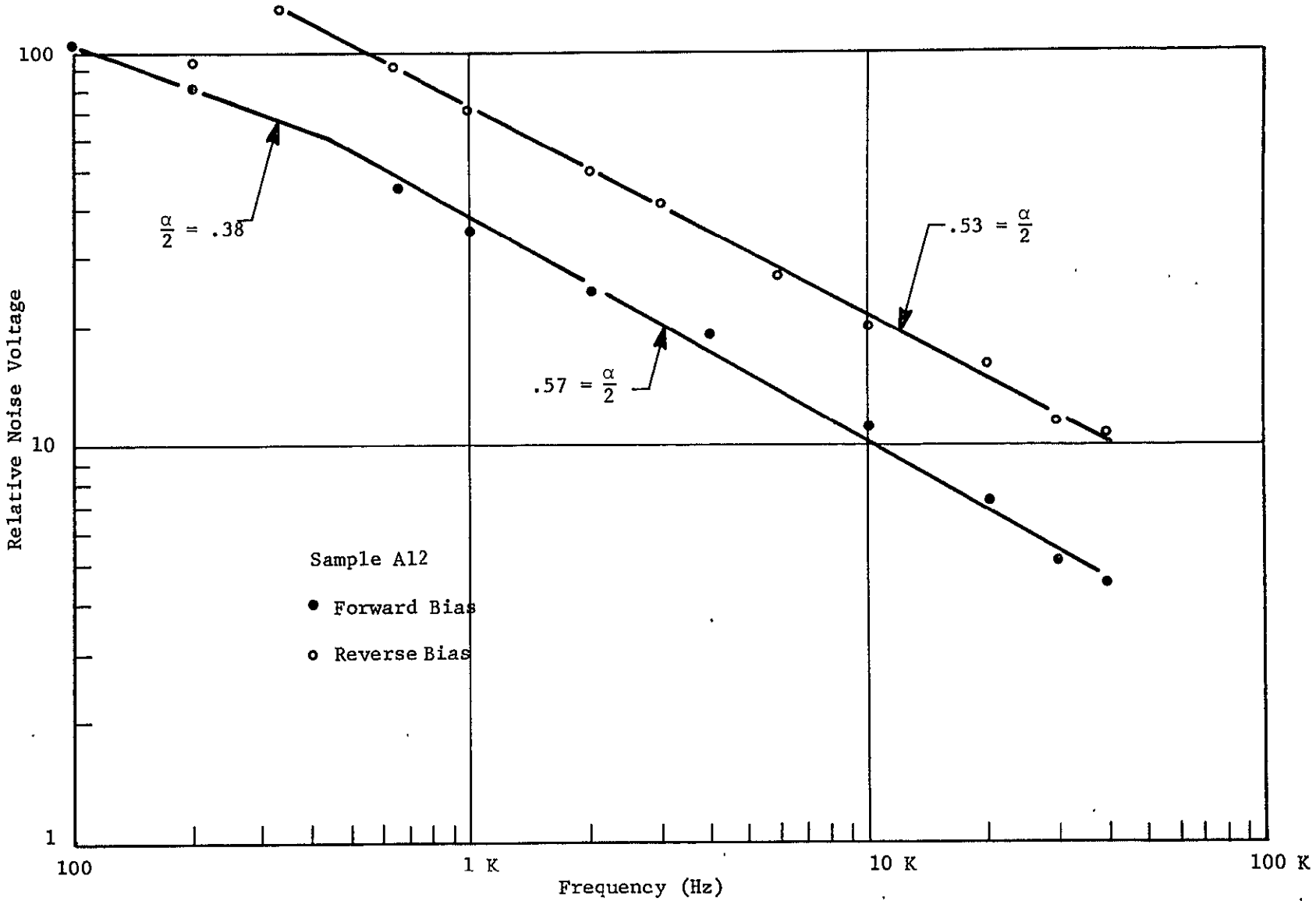

Figure 35 SAMPLE A12 DATA

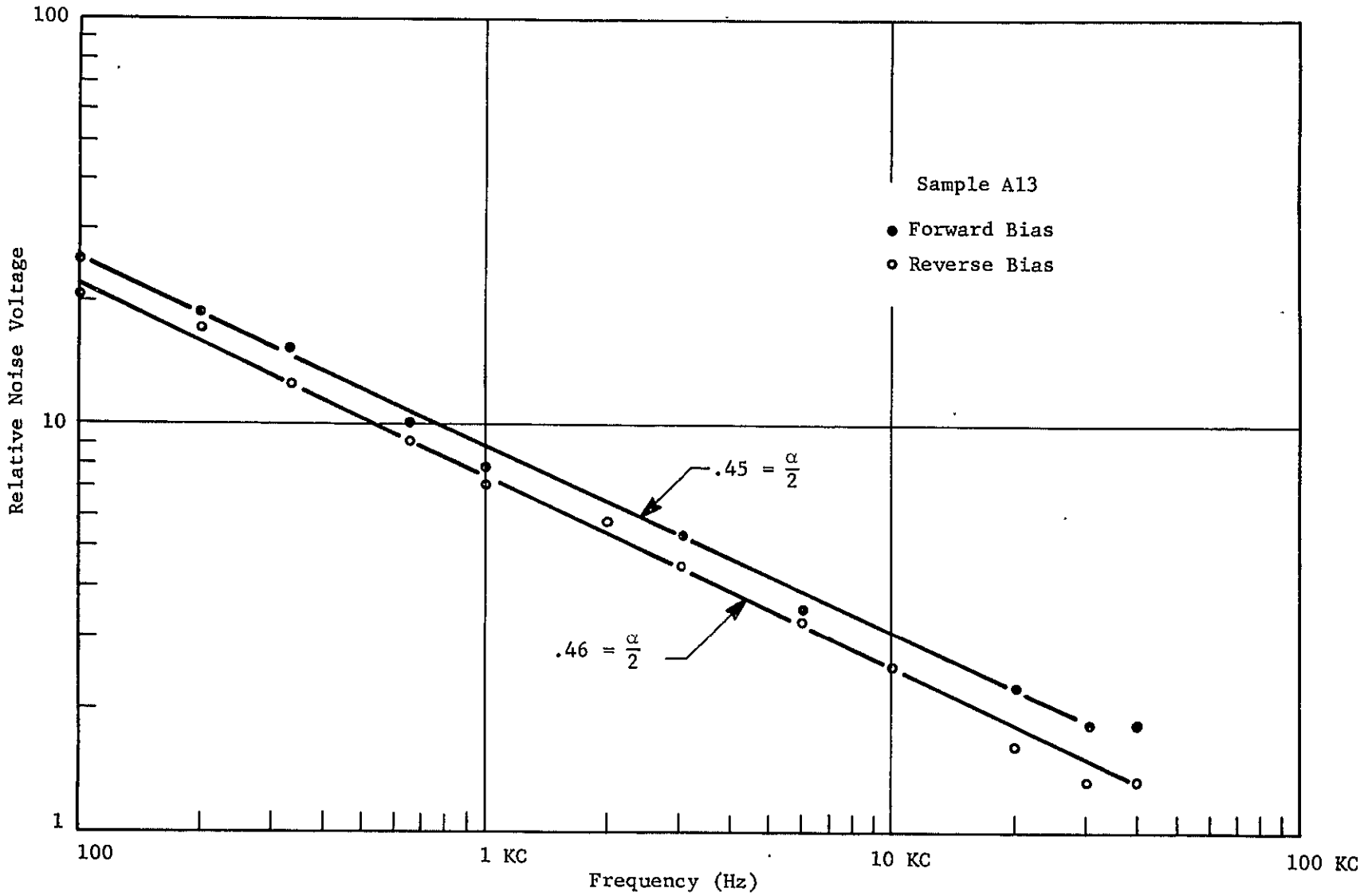

Figure 36 SAMPLE A13 DATA

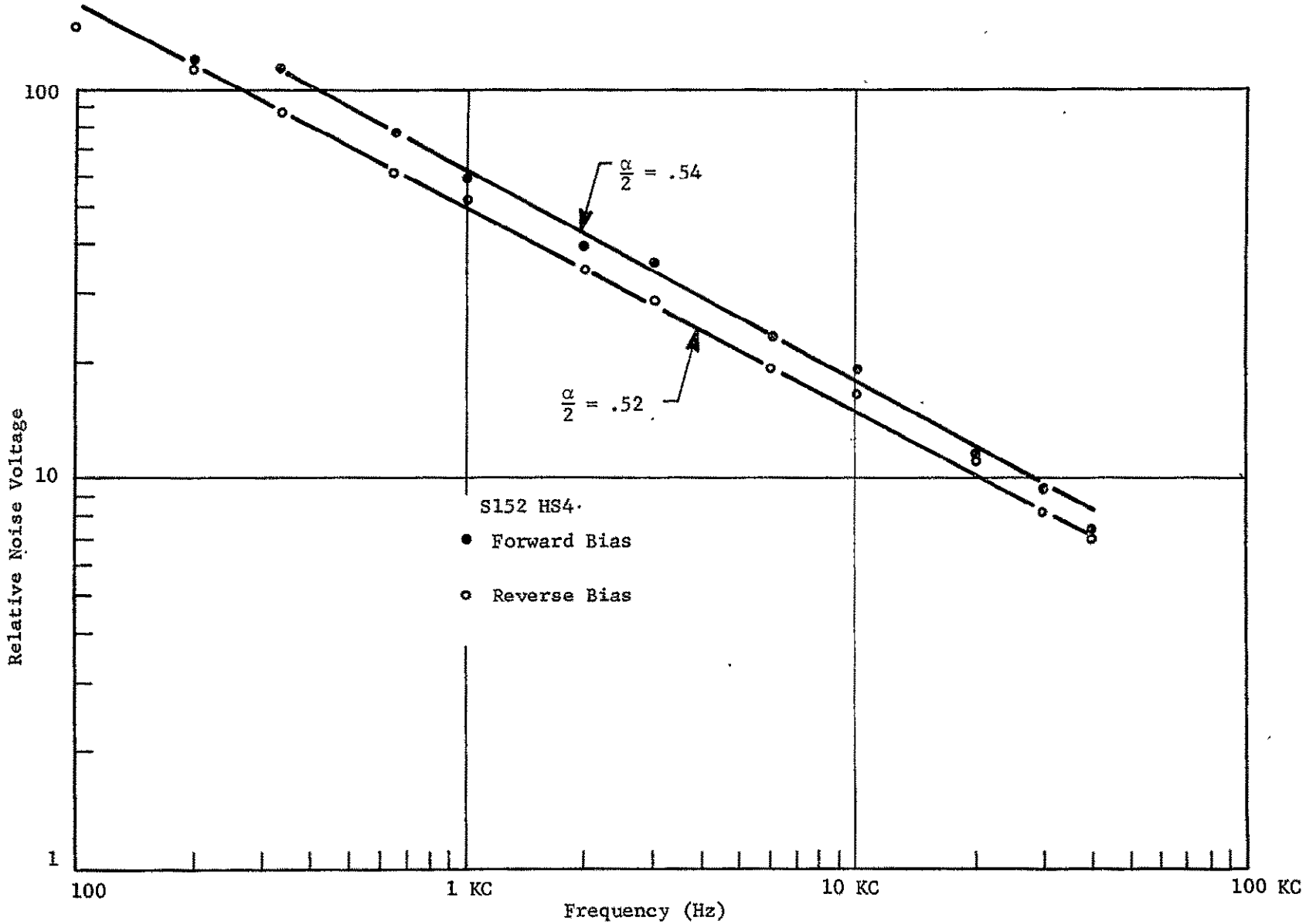

Figure 37 SAMPLE S152 HS4 DATA

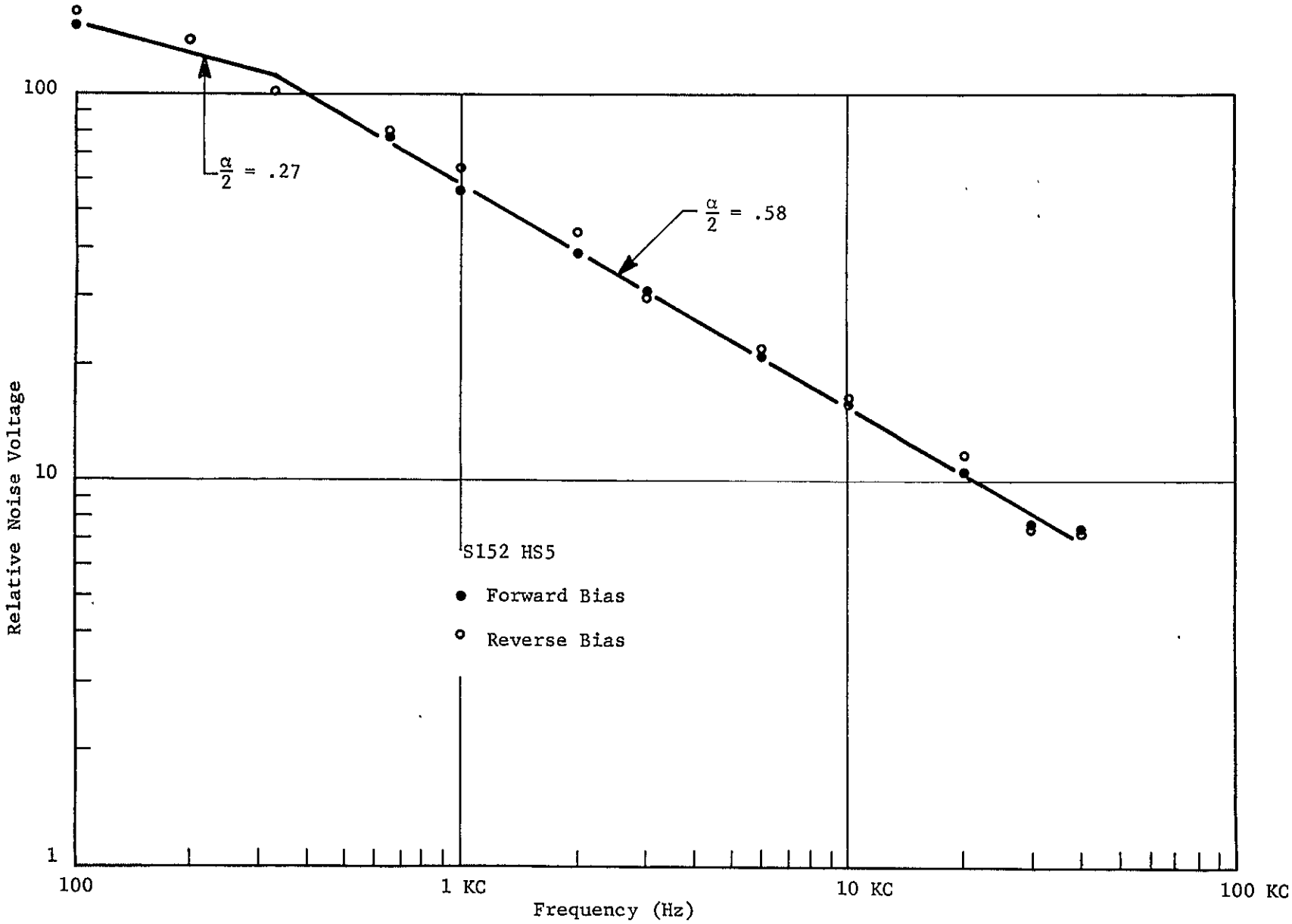

Figure 38 SAMPLE S152 HS5 DATA

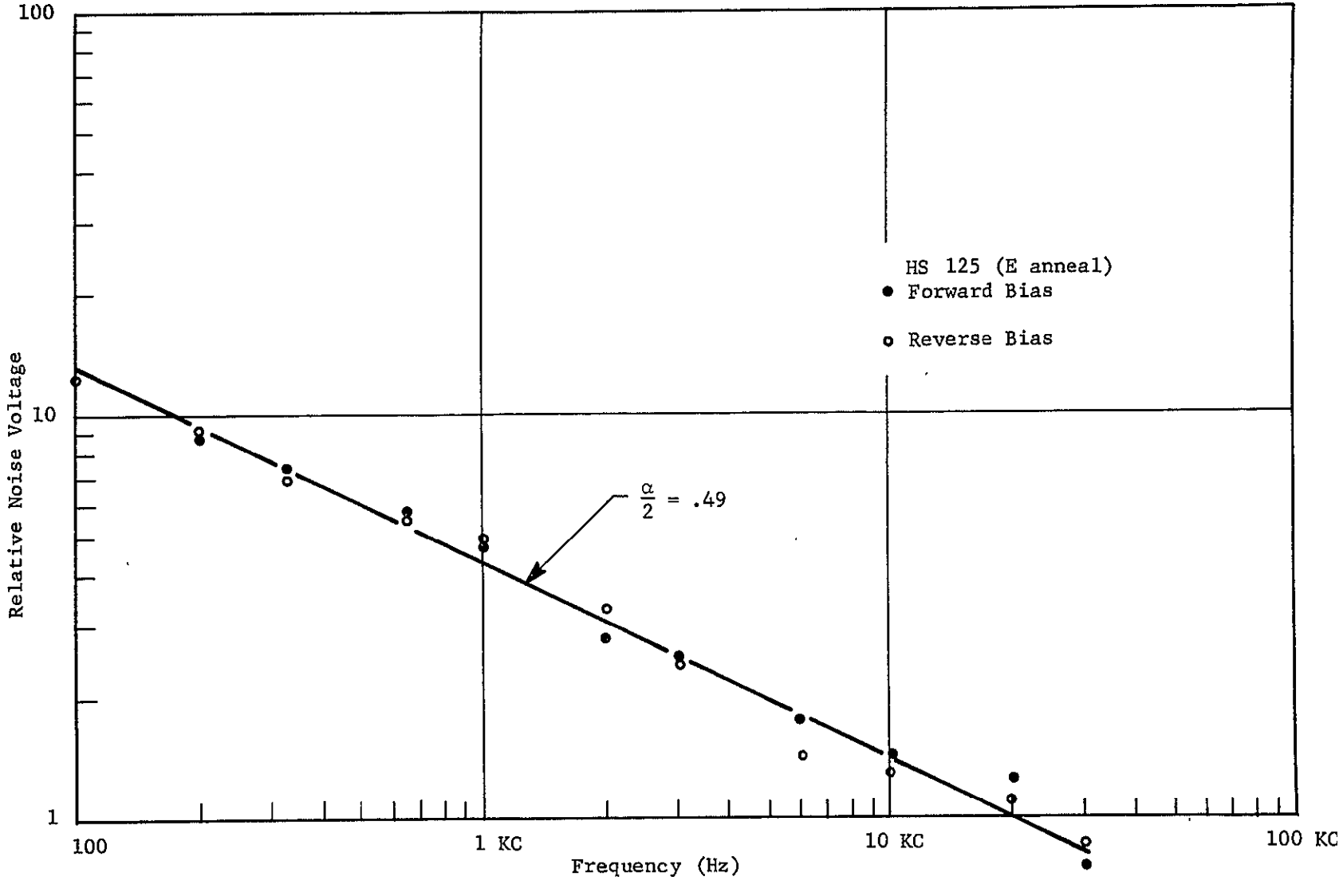

Figure 39 SAMPLE HS 125 (E_{ANNEAL}) DATA

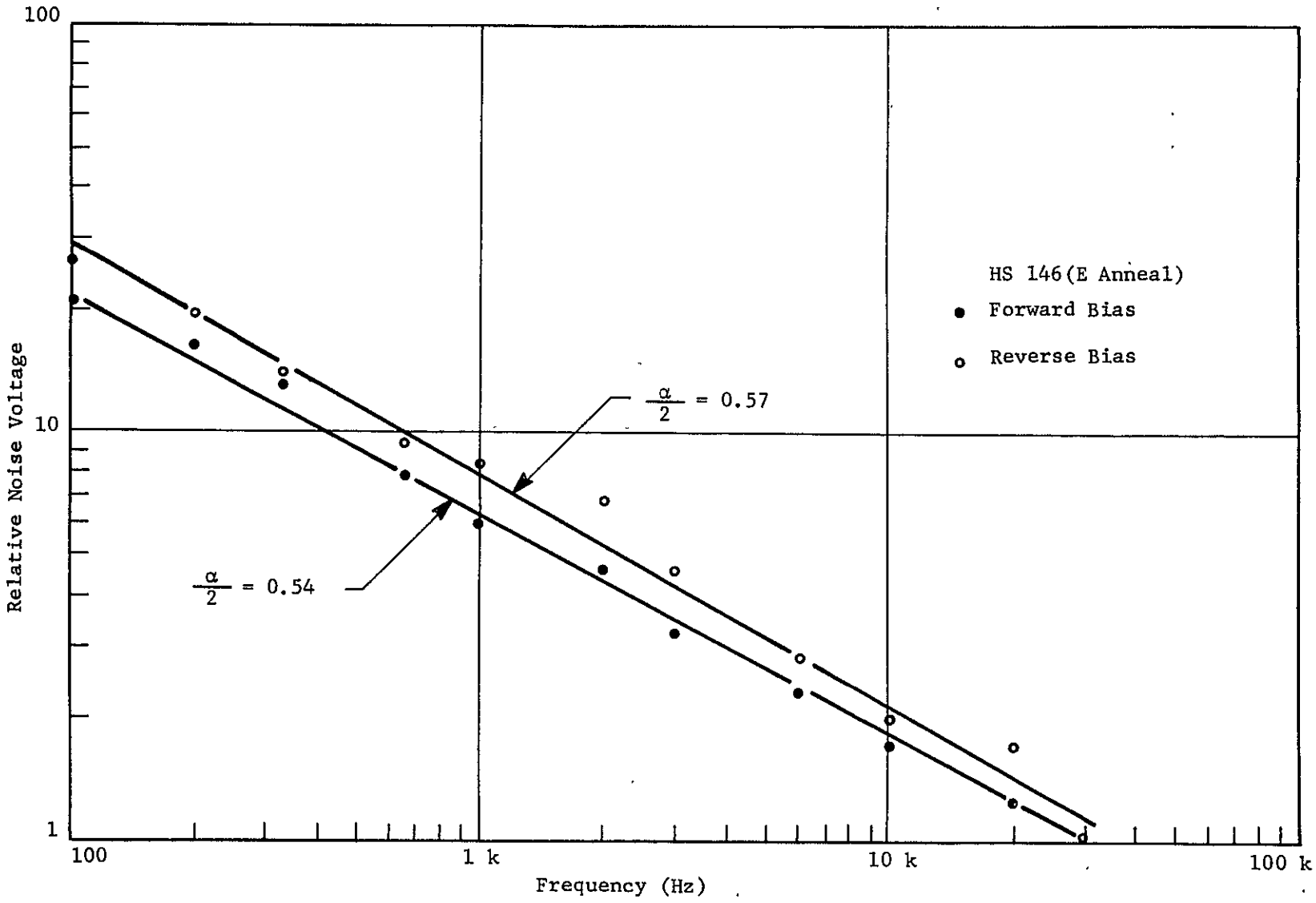

Figure 40 SAMPLE HS 146 (E_{ANNEAL}) DATA

well behaved curves being between 0.45 and 0.53. Samples A9, A10, A11, and A12 exhibit what may be described as a turnover or rolloff in either one or both bias directions. The majority of the four samples were found to be nonohmic (A9 was photovoltaic) and their resistance differed greatly with direction. We are uncertain at the present time as to the nonohmic nature of these high resistivity devices although we suspect that it arises from the difficulty of contacting to high ρ material.

C_1 was calculated for each sample tested and plotted as a function of ρ on a ρ vs C_1 graph as seen in Figure 41. All samples follow the $\rho^{5/2}$ curve well except for nonohmic samples A10, A12. This suggests that it may be difficult to correlate C_1 with ρ above 0.5 ohm-cm due to nonohmic contacts which do not give a true value of the material resistivity. A resistance read as a factor of 5 higher than that of bulk material would lower the calculated value for C_1 by a factor of 25 and "drop" all the data points above 0.5 ohm-cm into the C_1 vs $\rho^{5/2}$ curve. Also, both E annealed samples showed a lower C_1 than expected although it is difficult by their position on the C_1-ρ curve to determine to which part of the curve they belong. V-I curves showed them to be ohmic so that the region above 0.4 ohm-cm on a plot of C_1 vs ρ may be a mixture of nonohmic samples and ohmic excursions from the μm vs η graph. More work needs to be done in this area to understand the nature of high resistivity material and its relation to 1/f noise.

Noise spectra were taken at 0 bias for detectors A8, A9, and

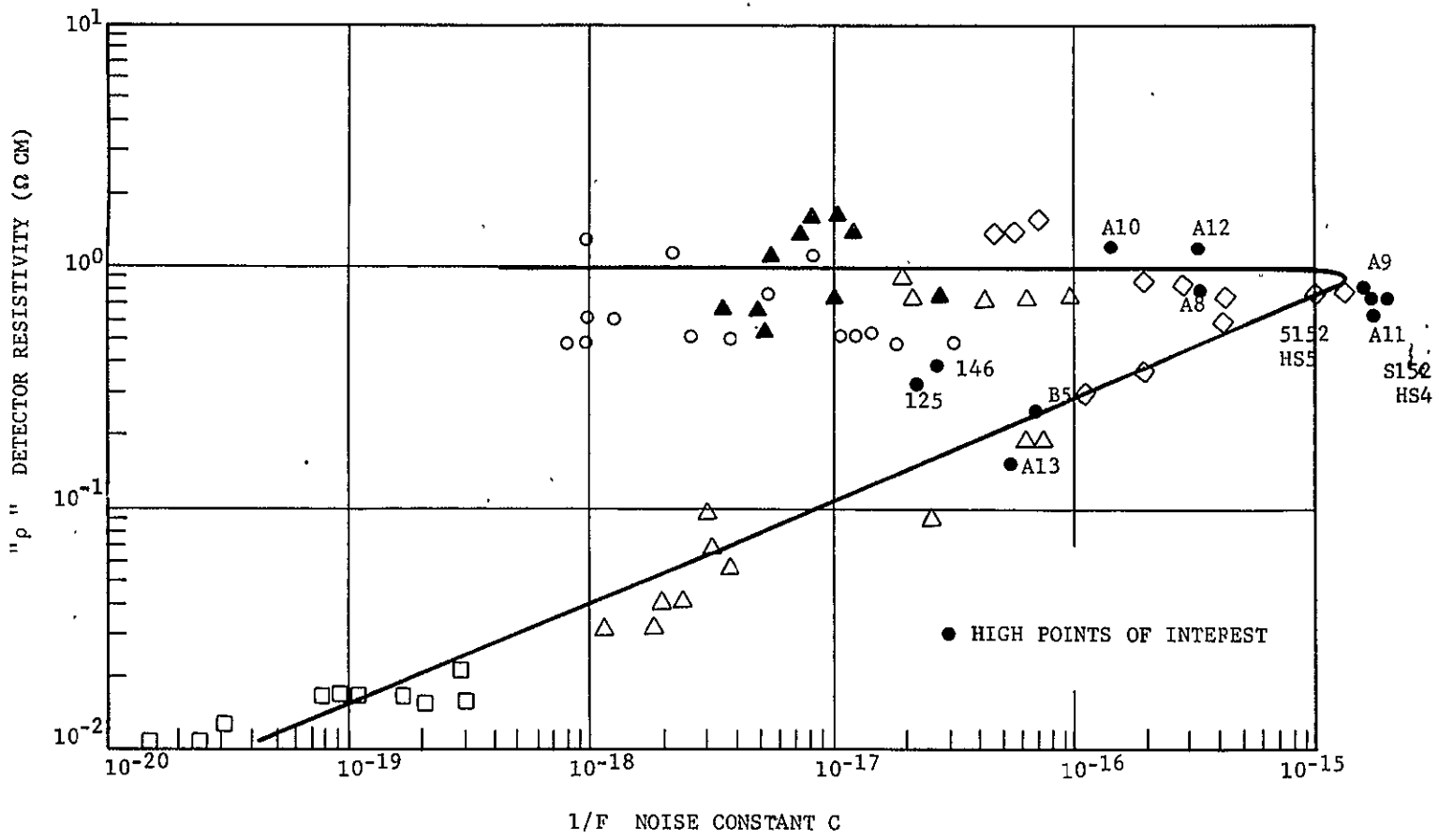

Figure 41 RHO VERSUS 1/f CONSTANT "C"

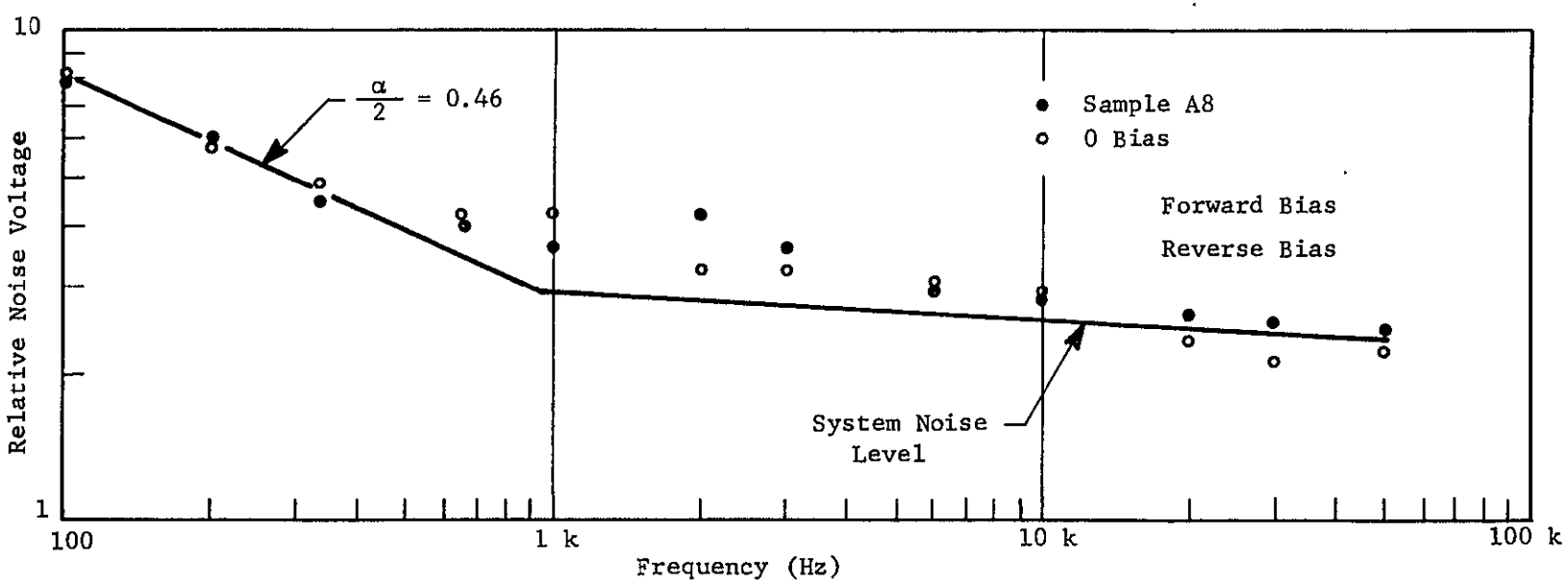

Figure 42 SAMPLE A8 DATA

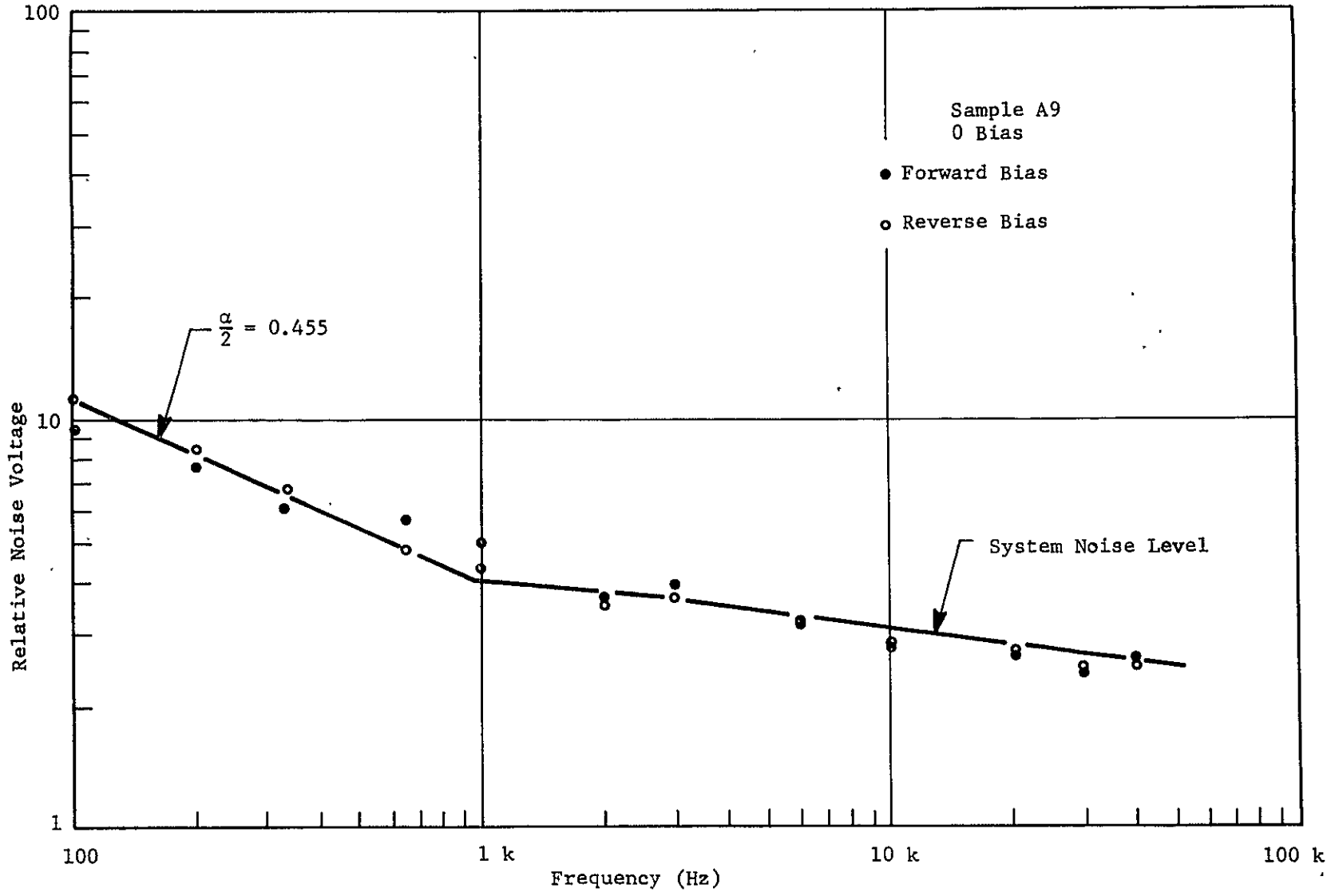

Figure 43 SAMPLE A9 DATA

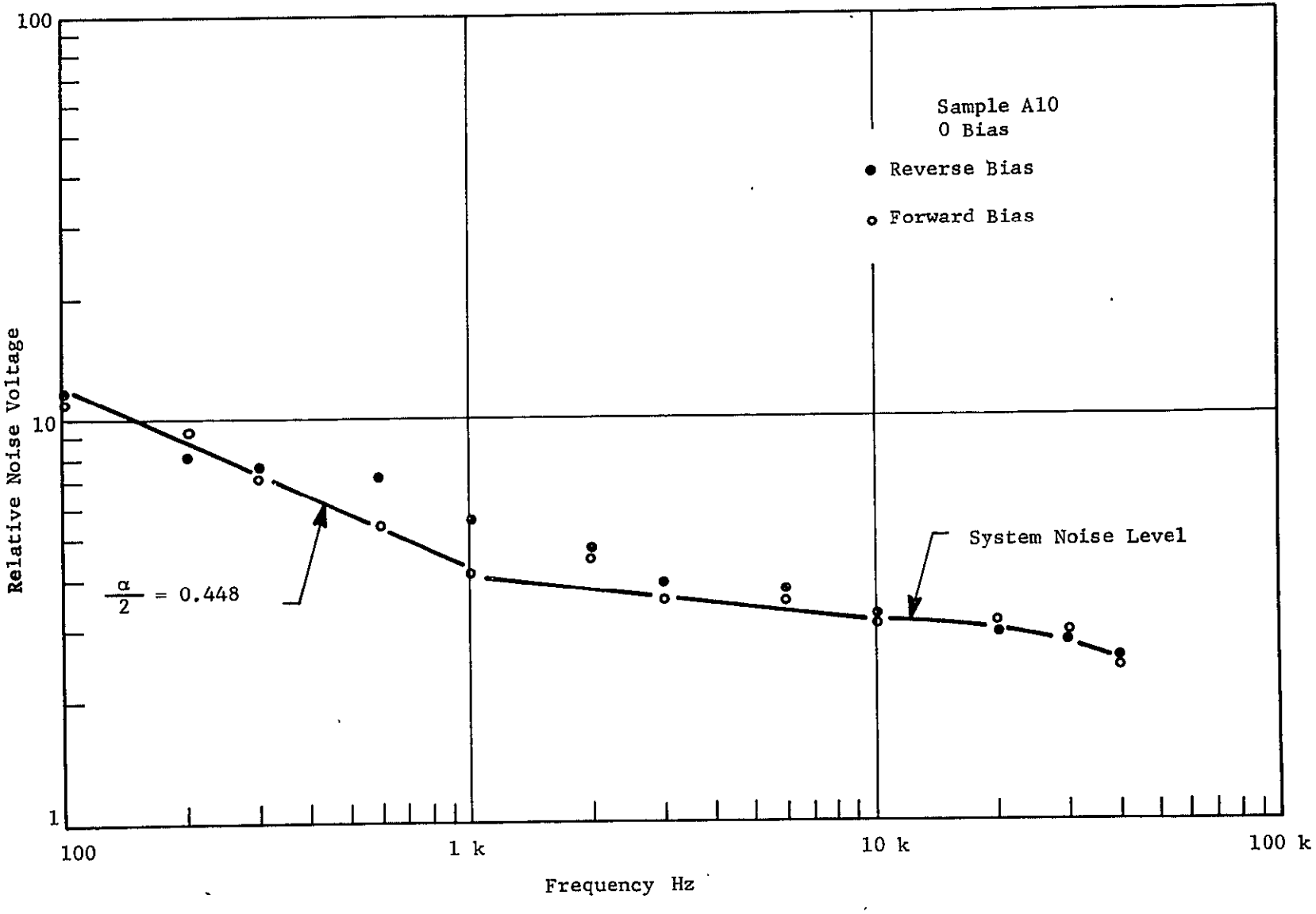

Figure 44 SAMPLE A10 DATA

at a slope of ≈ 0.45 is seen for all three samples. The detectors were replaced by equivalent carbon resistors and the 1/f noise disappeared indicating that it was truly detector noise. We believe that we see 1/f noise at zero bias due to the high C_1 of these samples and their nonohmic nature which supplies an electric field. However, the existence of this 1/f noise at 0 bias suggests that injecting current into a detector is not necessary to see 1/f noise.

SUMMARY

A summary of the results of this program may be outlined as follows:

a) The contacts of 15-micron (Hg,Cd)Te are not a source of 1/f noise, and although they may be nonohmic in high resistivity material, they still do not seem to contribute to the 1/f noise.

b) The existence of slow surface states in (Hg,Cd)Te and their effect on 1/f noise was not demonstrated, although driving carriers to the surface through the use of a magnetic field increased the 1/f noise.

c) Under standard test conditions, the 1/f noise coefficient in 15-micron (Hg,Cd)Te is related to sample resistivity when $\rho < 0.4$ Ω-cm.

d) The Hall mobility in 15-micron material has been noted to be related to carrier concentration such that high resistivity material has low carrier concentration and low mobility. This implies that

material parameters and 1/f noise may be strongly interrelated. In fact, the two excursions from the μ_H vs η curve (e annealed samples) showed a lower than expected 1/f noise coefficient for sample resistance.

e) 1/f noise at 77 °K was studied as a function of background temperature and the noise voltage level was found to remain constant although increased resistance at lower background temperature effectively lowered C_1. Cold shielded fields-of-view may therefore be an effective way to increase detector resistivity as well as performance.

f) 1/f noise was found at 0 bias current in nonohmic material suggesting that 1/f noise is not the result of bias current injection.

Problem Areas

The material inhomogeneity made comparisons across slabs and between adjacent slabs difficult. This hindered specifically the etch and anneal studies. This problem has been alleviated in that the two curves μ_H vs n and C_1 vs ρ may be used to characterize the effects of various treatments on material parameters and 1/f noise.

Discussion

The establishment of a strong correlation between resistivity, material parameters, and 1/f noise coefficient brings into question the nature of the material parameters of (Hg,Cd)Te. Although a

relationship between material parameters and 1/f noise suggests that the 1/f noise may be a bulk phenomena, the bulk parameters involved can be affected by surface conditions. Thus, a relationship between material parameters and 1/f noise may merely be a manifestation of surface effects. At the present time an understanding of the nature of the material parameters of (Hg,Cd)Te and its relation to the surface (especially the fast states) and 1/f noise seems to be vital to the ultimate reduction of 1/f noise in (Hg,Cd)Te.

Areas of future study should include:

a) The nature of the material parameters in (Hg,Cd)Te through the use of temperature dependent Hall data correlated with 1/f noise data.

b) Slab anneals to further study excursions from the n vs μ_H curve and their detective properties.

c) Further studies of the nature of the surface, specifically the density and characteristics of the fast states and their relation to 1/f noise.

REFERENCES

1) Van der Ziel, Physica 16, 359 (1950).
2) Firle & Winston, J. Appl. Phys. 26, 716, (1955).
3) B.V. Rollin & I. Templeton, Proc. Phys. Soc. (London) B66, 250 (1953).
4) F.J. Hyde, Proc. Phys. Soc. (London) B69 242 (1956).

5) L. Bess, Phys. Rev. 103, 72, (1956).
6) T.G. Maple, L. Bess, and H.A. Gebbie, J. Appl. Phys. 26, 190 (1955).
7) L. Bess & L.S. Kisner, J. Appl. Phys. 37, 3458 (1966).
8) H.C. Montgomery, Bell System, Tech. J. 31 950, (1952).
9) J.J. Brophy and N. Rastoker, Phys. Rev. 100, 754 (1955).
10) A.U. MacRae and H. Levinstein, Phys. Rev. 119, 62, (1960).
11) T.G. Maple, L. Bess, and H.A. Gebbie, J. Appl. Phys. 26, 490 (1955).
12) J.J. Brophy, Phys. Rev. 111, 1050 (1958).
13) P. Kruse, L. McGlauchlin, and R. McQuiston, Elements of Infrared Technology, Wiley and Sons, New York 1962.
14) A.L. McWharten, Semiconductor Surface Physics, R.H. Kingston et al eds Philadelphia.
15) L. Bess, Phys. Rev. 91, 1569 (1953).
16) L. Bess, Phys. Rev. 103, 72 (1956).
17) S.R. Morrison, Phys. Rev. 104, 619 (1956).
18) O. Jantsch, Solid State Electron, 11, 267 (1968).
19) O. Jantsch and I. Feight, Phys. Rev. Lett. 23, 912 (1969).
20) C.T. Sah and F.H. Hielscher, Phys. Rev. Letts., 17, 956 (1966).
21) A.U. MacRae, J. Appl. Phys. 33, 2570 (1962).
22) A.U. MacRae and H. Levinstein, Phys. Rev. 119, 62 (1960).
23) A.N. Kohn & J.J. Schlickman, "(Hg,Cd)Te Detector for 14-16 Micron Spectral Band" (Confidential), Final Report NASA Langley Research Center, June 1968.
24) H. Suhl, Bell Syst. Tech. J. 32 647 (1953).